Non-Abelian color fields from relativistic color charge configurations in the classical limit

W. Cassing,[1] V. V. Goloviznin,[2] S. V. Molodtsov,[3,4] A. M. Snigirev,[5] V. D. Toneev,[3] V. Voronyuk,[2,3] and G. M. Zinovjev[2]

[1]*Institute for Theoretical Physics, University of Giessen, 35392 Giessen, Germany*
[2]*Bogolyubov Institute for Theoretical Physics, National Academy of Sciences of Ukraine, 252143 Kiev, Ukraine*
[3]*Joint Institute for Nuclear Research, 141980 Dubna, Moscow Region, Russia*
[4]*Institute of Theoretical and Experimental Physics, 117218 Moscow, Russia*
[5]*Skobeltsyn Institute of Nuclear Physics, Lomonosov Moscow State University, 119991 Moscow, Russia*

We study the dynamics of color fields as generated by simple configurations of relativistic particles with Abelian and non-Abelian [SU(2)] charges in the classical limit. We find that chromodynamic (non-Abelian) systems generally show Coulomb-like features by analogy with electrodynamics. A peculiar feature in the non-Abelian case is the additional strength of the chromoelectric and chromomagnetic fields caused by the contribution of changing the color charge. This change of color SU(2) charges results in a rotation of the color vector, which is getting very fast at close partonic distances. The presence of this non-Abelian additional term in the chromoelectric and chromomagnetic fields creates a color charge glow, which is manifested as a distinct color wave disturbance arising due to the finite distance at which the color interaction becomes active. This situation may be relevant to the hadronization phase in ultrarelativistic heavy-ion collisions, where the partonic state is governed by strong local color fluctuations.

I. INTRODUCTION

Ultrarelativistic nucleus-nucleus collisions at Relativistic Heavy-Ion Collider (RHIC) or Large-Hadron-Collider (LHC) energies provide an opportunity to explore strongly interacting QCD matter in and out of equilibrium. The experiments at the RHIC and the LHC have demonstrated that a stage of partonic matter is produced in these reactions that is in approximate equilibrium for a couple of fm/c [1–5]. Contrary to early expectations, guided by perturbative QCD (pQCD) calculations, the medium shows a collective response of the strongly interacting plasma (sQGP) with interaction rates beyond those of high density hadronic matter [6–8]. In fact, viscous hydrodynamical calculations are successful in describing the collective response of the partonic medium, which is dominantly reflected in the differential azimuthal angular distribution of the final (observable) hadrons [9–11]. These angular distributions can be characterized by the Fourier coefficients v_n that specify the strength of the nth harmonics in the angular distributions. The observation of sizable uneven coefficients v_3, v_5 showed the presence of initial-state fluctuations, which are due to random positions of the nucleons in the targets and random inelastic hard interactions in the primary phase of the nucleus-nucleus collisions or due to color field fluctuations in an early glasma phase. This comes about as follows: the passage time of even central Au + Au (or Pb + Pb) at RHIC energies is not longer than 0.2 fm/c at top RHIC energies and below 0.02 fm/c at the present LHC energies. During these short times the wave functions of the nucleons in the target are frozen and even the partonic wave functions of the individual nucleons are approximately frozen so that configurations with high fluctuations in the energy density show up in individual events [12–16]. In fact, when accounting for such initial-state fluctuations, all harmonics v_n in the azimuthal angular distributions can be described in event-by-

event calculations within the hydrodynamic framework [17] or within transport approaches like the parton-hadron-string dynamics (PHSD) theory [18].

The partonic medium (near an equilibrium state) is characterized by a very low ratio of the shear viscosity to the entropy density $\eta/s \approx 0.1$–0.2, which is close to the lower bound of $1/(4\pi)$ [19]. It is presently accepted that η/s has a minimum as a function of temperature close to $T_c \approx 160$ MeV and increases fast in the hadronic phase, i.e., with decreasing temperature [20–22]. Furthermore, the ratio of the bulk viscosity to entropy density is expected to have a maximum close to T_c [23–25].

However, the (dissipative) hydrodynamic calculations start at delayed times of 0.2–1.0 fm/c from the initial impact of the heavy ions since approximate equilibrium has to be achieved by presently unknown mechanisms [26]. Initial fluctuations in the hydrocalculations are usually imposed by independent Glauber model simulations. Initial conditions very similar to the Glauber model are included by default in the PHSD transport approach that has been tested successfully so far for a variety of observables in nucleus-nucleus collisions from lower super-proton-synchrotron (SPS) up to LHC energies [27–30], including electromagnetic probes such as e^+e^- or $\mu^+\mu^-$ pairs [31]. The event-by-event PHSD calculations for heavy-ion reactions from RHIC to LHC energies show that apart from local fluctuations in the energy density also sizable fluctuations in color occur although the total system is always color neutral. Furthermore, the formation of color dipoles is observed in the microscopic transport calculations, in particular in the hadronization phase at rather low parton densities, which implies that color forces might play an important role during the early nonequilibrium stage (cf. Ref. [32]) as well as in the dynamics of hadronization.

The dynamical evolution of such systems depends on the initial conditions for the above-noted string-like mechanism and additionally on the parton distribution function in the

nuclei prior to the collision. High-energy heavy-ion collisions initially release a large number of gluons from their wave functions. In fact, the wave function of a hadron boosted close to the light cone is densely packed with gluons so that they may overlap leading to saturation in the gluon density due to nonlinear gluon interactions [33]. Therefore, at high collision energies the colliding hadrons can be viewed as high-density gluon fields. This dense system is nowadays referred to as a color glass condensate (CGC) (cf. the review articles [34]).

The problem of computing the distribution functions for gluons at very small Bjorken x has been a task for decades [34]. The gluon and quark distribution functions are computable in perturbation theory at large values of the Bjorken x, but at small x the precise computation encounters much uncertainty. The perturbative paradigm of the low x gluon physics is the Balitsky-Fadin-Kuraev-Lipatov (BFKL) equation [35], which, however, is linear and ignores mutual interactions of the gluons. Thus, nonperturbative calculations are needed. The nuclear structure function for large parton density at small x, where classical methods are applicable, is rather successfully described by the McLerran-Venugopalan model [36] within a classical effective field theory approach, where the degrees of freedom are static color sources in the hadron at large x, coupled to the dynamical gluon fields at small x. It recently has been shown that renormalization group generalization of this effective action can improve this approach. The renormalization group equations, derived by requiring that observables are independent of the separation in x between sources and fields, lead to an infinite hierarchy of evolution equations in x. With appropriate initial conditions, the solutions of this Jalilian-Marian, Iancu, McLerran, Weigert, Leonidov, and Kovner (JIMWLK) hierarchy [37] allow one to compute a wide range of multiparticle final states in deeply inelastic scattering or/and hadronic collisions and to reproduce several key results in small x QCD.

If a single heavy nucleus (such as Au or Pb) is considered within the McLerran-Venugopalan model [36], an ultrarelativistic collision of two such nuclei at the very early times can be treated as a collision of CGC sheets, which are sources of the Yang-Mills radiation. The equations that describe the color field evolution were applied to RHIC energy collisions of nuclei and deuteron-Au reactions [38]. This intermediate matter is highly coherent and responsible for the transition from CGC to the quark-gluon plasma where fast thermalization might be reached due to field instabilities. This intermediate state is called the glasma, which is gluon rich and low in the quark/antiquark density.

One should emphasize that the CGC picture refers to the very early interaction stage of ultrarelativistic collisions. To validate this picture—by comparing its predictions with experiment—the glasma model has to be supplemented by hydrodynamic or kinetic models that transport the energy density and its fluctuations to the final hadronic spectra. Both model types as well as the matching procedure, connecting the two different descriptions of the system evolution, introduce additional uncertainties, which prevent unambiguous conclusions, especially in the case of nucleus-nucleus collisions. In particular, the flow harmonics, being sensitive to the early stage of the reaction, have been compared using the CGC

and Glauber initial conditions. Both model versions, being progressively developing [39,40], give very close results with a small advantage in favor of one or another initial condition in different studies. The first LHC data on the bulk particle production in Pb + Pb collisions are in good agreement with improved CGC expectations but they are also compatible with Monte Carlo event generators. Both approaches have in common that they include strong coherence effects. Exhaustive analysis of forthcoming more differential observables is needed to better discriminate between the models (cf. [41,42]).

Our present study is, furthermore, motivated by recent investigations of peripheral ultrarelativistic heavy-ion collisions at the RHIC and the LHC, for which a large electric charge eZ of the colliding nuclei leads to the generation of intense electric and magnetic fields during the passage time of the charged spectators, as discussed in Ref. [43]. It is speculated that a very strong electromagnetic field of short duration essentially in the preequilibrium phase might have an important impact on particle production [44,45].

Future ALICE measurements are promising to provide an answer to these questions and, possibly, to strengthen the standard approach to the saturation physics [34] treating the gluon fields and the corresponding scattering cross sections classically (rapidity-independent). Such classical field dynamics calls for a transport formulation and the development of an extended transport code for ultrarelativistic collision processes, including the color dynamics of the gluon fields (beyond the processes implemented, e.g., in PHSD).

In order to proceed to a solution of this task, we are going here to give practical estimates for the space-time dependence of classical non-Abelian fields, which (in line with PHSD) are generated by colored quarks in relativistic heavy-ion collisions. In this respect we will develop an instrumental approximation for configurations of two color charges, a color charge and a color dipole, and two color dipoles, which are moving along a straight line towards each other. For our initial study of non-Abelian fields we simplify the problem to the SU(2) color group. We recall that such color configurations are just the elementary basic examples in ultrarelativistic heavy-ion collisions in the existing phenomenological models [27,46]. The classical character of the non-Abelian field means, as usual, that the field operators are replaced by their average values for the quantum state, and the off-diagonal elements are neglected. Quarks are treated as classical pointlike massive particles possessing a color charge. We will estimate the characteristic values of the classical gluon field strength but are not interested in the parton (gluon) distribution functions themselves. More precisely, we will specify the features characteristic of the non-Abelian nature of fields in comparison to solutions for Abelian fields for the same coupling strength.

The actual layout of our study is as follows. In Sec. II, we first recall the results from classical (Abelian) electrodynamics considering the retarded electromagnetic field created by a moving source. In Sec. III, the particularities of the non-Abelian color field produced by a color source are discussed on the basis of an approximate solution of the classical Yang-Mills equations. The application of this technique to particular cases of two color charges, a charge-color dipole

system and two dipoles moving in the opposite direction is presented in Secs. IV–VI, respectively. Our conclusions are given in Sec. VII. Some more technical details for the color interactions and the construction of approximate solutions of the classical Yang-Mills equations are shifted to the Appendix.

II. FIELD OF A RELATIVISTIC ABELIAN CHARGE

In this section, we recall the results from classical electrodynamics: The field of a pointlike charge propagating along the trajectory $r(t)$ is described by the (retarded) Liénard-Wiechert potential at the observation point r_0

$$\varphi = \frac{1}{4\pi} \left[\frac{e}{R - vR} \right]_{t'}, \quad A = \frac{1}{4\pi} \left[\frac{ev}{R - vR} \right]_{t'}. \quad (1)$$

Throughout the paper we stick to the standard system of units with speed of light $c = 1$, dimensionless electrodynamic e and non-Abelian g charges, i.e., have the proper factors of $\hbar c$ to keep the proper dimensions. Then characteristic distances in the problem are of an order of one Fermi and the potentials and field strengths are measured in units of m_π and m_π^2, respectively, where m_π is the π-meson rest mass. In Eq. (1), φ is the zeroth component of the potential and A is its vector component, v is the particle velocity at some retarded time t', which is determined by the distance between the observation point and the particle $R = |R|$ where $R = r_0 - r(t')$ is the radius vector from the charge position to the observation point r_0. It is of importance to note that the relation between the retarded and laboratory time t is

$$R = t - t', \quad (2)$$

(although the notation R' would be more suited). The electric and magnetic fields are then given by

$$E = -\frac{\partial A}{\partial t} - \nabla \varphi, \quad H = \nabla \times A. \quad (3)$$

Using Eq. (2) we get

$$\frac{\partial A}{\partial t} = \frac{\partial A}{\partial t'} \frac{\partial t'}{\partial t}, \quad \nabla \times A = \nabla \times \varphi v,$$

$$\frac{\partial t'}{\partial t} = \frac{1}{1 - vn}, \quad \nabla t' = -\frac{n}{1 - vn}, \quad \nabla R = \frac{n}{1 - vn},$$

$$\nabla(vR) = v - \frac{n}{1 - vn}(\dot{v}R - v^2)\nabla \times v$$

$$= \nabla t' \times \frac{\partial v}{\partial t'} = -\frac{n}{1 - vn} \times \dot{v} \quad (4)$$

with the unit vector $n = R/R$ while $\dot{v} = \partial v/\partial t'$ is the particle acceleration retarded in time (see Ref. [47]). Combining these relations and using the potentials from Eq. (1) we get the following results for the electric and magnetic fields:

$$E = \frac{1}{4\pi} \left[\frac{e}{R^2} \frac{(1 - v^2)(n - v)}{(1 - vn)^3} + \frac{e}{R} \frac{n \times (n - v) \times \dot{v}}{(1 - vn)^3} \right]_{t'},$$

$$H = \frac{1}{4\pi} \left[-\frac{e}{R^2} \frac{n \times v}{(1 - vn)^3}(1 - v^2 + \dot{v}R) - \frac{e}{R} n \times \dot{v} \right]_{t'}$$

$$= n \times E. \quad (5)$$

In fact the formulas (convenient for practical purposes) express the electric and magnetic fields as a function of the particle trajectory (at $\dot{v} = 0$) at the current time $r = r_0 - r(t)$ in the form

$$E = \frac{1}{4\pi} \frac{er(1 - v^2)}{[(rv)^2 + r^2(1 - v^2)]^{3/2}}, \quad H = v \times E. \quad (6)$$

We also recall that the potentials can then be written as

$$\varphi = \frac{1}{4\pi} \frac{e}{[(rv)^2 + r^2(1 - v^2)]^{1/2}},$$

$$A = \frac{1}{4\pi} \frac{ev}{[(rv)^2 + r^2(1 - v^2)]^{1/2}}. \quad (7)$$

III. FIELD OF RELATIVISTIC SU(2) CHARGES (CLASSICAL YANG–MILLS FIELDS)

In order to keep our approach transparent, we consider here SU(2) non-Abelian fields only. In the classical approximation they are c-number functions, which are the solutions of the classical Yang-Mills equations. We analyze the QCD Lagrangian of the form

$$\mathcal{L} = -\tfrac{1}{4}\widetilde{G}^{\mu\nu}\widetilde{G}_{\mu\nu} - \widetilde{j}^\mu \widetilde{A}_\mu, \quad (8)$$

where the color vector $\widetilde{A}_\mu = (A_\mu^1, A_\mu^2, A_\mu^3)$ represents a triplet of the Yang-Mills fields of different colors (isospin), $\widetilde{j}^\mu$ is the current density of external color sources, and $\widetilde{G}_{\mu\nu} = \partial_\mu \widetilde{A}_\nu - \partial_\nu \widetilde{A}_\mu + g \widetilde{A}_\mu \times \widetilde{A}_\nu$ is the gluon field tensor with the covariant derivative acting as $\widetilde{D^\mu f} = \partial^\mu \widetilde{f} + g\widetilde{A}^\mu \times \widetilde{f}$. The product sign $\times$ corresponds to the vector product in the color space. The classical equations of motion, as known, then read

$$\widetilde{D^\mu G_{\mu\nu}} = \widetilde{j}_\nu. \quad (9)$$

The most significant difference between these equations and the electrodynamic equations is the compatibility conditions of the system of Eqs. (9)

$$\widetilde{D^\mu j_\mu} = 0, \quad (10)$$

which generally implies that the color vector charge is not conserved in a sense similar to electrodynamics. Then as a suitable solution of the Yang-Mills equations for a single particle with constant color charge $\widetilde{C}$ one may take the potentials of the form

$$\widetilde{\varphi} = \frac{1}{4\pi} \left[\frac{\widetilde{C}}{R - vR} \right]_{t'}, \quad \widetilde{A} = \frac{1}{4\pi} \left[\frac{\widetilde{C}v}{R - vR} \right]_{t'}. \quad (11)$$

Similarly to the electromagnetic case, discussed above in Sec. II, $R = r_0 - r(t')$ is the radius vector directed from the charge position to the observation point r_0. In electrodynamics one can easily verify the uniqueness of the solutions (1) for a pointlike charge (taking into account the well-known problem of the singularity associated with the self-interaction [48]) because the superposition principle for solutions remains valid. Furthermore, the general form of the retarded solution is well known. In the non-Abelian case, we cannot benefit from an analysis of the general Yang-Mills solutions but one can construct approximate solutions with properties similar to the solutions of electrodynamics. As mentioned above, here

we focus on the analysis of some simple examples important for practical applications treating the relativistic color objects propagating along a straight line.

As an approximate solution, we consider a superposition of the Liénard-Wiechert potentials (11) in which the vector of the particle color charge can change in time and should be taken at the retarded time, which results exactly from the general form of the retarded solution as

$$\widetilde{\varphi}(\boldsymbol{r},t) = \frac{1}{4\pi}\int \frac{\widetilde{\rho}(\boldsymbol{r}',t')\delta(t-t'-|\boldsymbol{r}-\boldsymbol{r}'|)}{|\boldsymbol{r}-\boldsymbol{r}'|}d^3r'dt',$$

$$\widetilde{\boldsymbol{A}}(\boldsymbol{r},t) = \frac{1}{4\pi}\int \frac{\widetilde{\boldsymbol{j}}(\boldsymbol{r}',t')\delta(t-t'-|\boldsymbol{r}-\boldsymbol{r}'|)}{|\boldsymbol{r}-\boldsymbol{r}'|}d^3r'dt'.$$

$$(12)$$

As an example, we consider a simple approximation of the covariant four-current with the delta function for a pointlike particle

$$\widetilde{j}_\mu(\boldsymbol{r}',t') = (\widetilde{C}\delta(\boldsymbol{r}'-\boldsymbol{r}(t)), \widetilde{C}\boldsymbol{v}(t)\delta(\boldsymbol{r}'-\boldsymbol{r}(t))), \qquad (13)$$

where $\boldsymbol{v}(t) = \dot{\boldsymbol{r}}(t)$ is the particle velocity. In this context the compatibility condition (10) for a pointlike charge becomes

$$\dot{\widetilde{C}} = g[\widetilde{\varphi}(t,\boldsymbol{r}) - \boldsymbol{v}\widetilde{A}(t,\boldsymbol{r})] \times \widetilde{C}. \qquad (14)$$

From these equations it is easy to see that the modulus of the color charge vector remains constant. One should note that in this approximation of color field sources as pointlike charges the evolution of a separate parton is described by Eq. (14) due to the continuity equation. Moreover, in the developed consideration, as noted in the Introduction of Ref. [37], there is a separation of scales. However, even in the tree approximation the strength of the generated field may be so high that its influence on the particle (parton) trajectory should be taken into account. Presently available transport codes, in particular the PHSD, allow one to consider this effect and to get a consistent picture at the cost of an essential simplification of the problem.

In the following we take the color charge as a unit vector and specify the magnitude of the charge to be given by the coupling constant g [$\alpha_g = g^2/(4\pi) = 0.3$], thus taking the coupling strength out as an independent factor. This approximation will be justified below in more detail.

The consideration of the non-Abelian charge as a function of time leads to the generation of additional terms in the expressions for the chromoelectric and chromomagnetic fields of color pointlike charges, which stem from the derivative of the color charge vector with respect to the retarded time t', i.e.,

$$\widetilde{D} = \frac{\partial \widetilde{C}}{\partial t'}, \quad \frac{\partial \widetilde{C}}{\partial t} = \widetilde{D}\frac{\partial t'}{\partial t}, \quad \nabla\widetilde{C} = \widetilde{D}\nabla t',$$

$$\nabla \times \widetilde{C}\boldsymbol{v} = \nabla t' \times \widetilde{D}\boldsymbol{v} + \nabla t' \times \widetilde{C}\frac{\partial \boldsymbol{v}}{\partial t'}.$$

The results for the non-Abelian chromofields are

$$\widetilde{\boldsymbol{E}} = \frac{1}{4\pi}\left[\frac{\widetilde{C}}{R^2}\frac{(1-v^2)(\boldsymbol{n}-\boldsymbol{v})}{(1-\boldsymbol{v}\boldsymbol{n})^3} + \frac{\widetilde{C}}{R}\frac{\boldsymbol{n}\times(\boldsymbol{n}-\boldsymbol{v})\times\dot{\boldsymbol{v}}}{(1-\boldsymbol{v}\boldsymbol{n})^3}\right.$$

$$\left.+ \frac{\widetilde{D}}{R}\frac{\boldsymbol{n}-\boldsymbol{v}}{(1-\boldsymbol{v}\boldsymbol{n})^2}\right]_{t'}$$

$$\widetilde{\boldsymbol{H}} = \frac{1}{4\pi}\left[-\frac{\widetilde{C}}{R^2}\frac{\boldsymbol{n}\times\boldsymbol{v}}{(1-\boldsymbol{v}\boldsymbol{n})^3}(1-v^2+\dot{\boldsymbol{v}}R) - \frac{\widetilde{C}}{R}\boldsymbol{n}\times\dot{\boldsymbol{v}}\right.$$

$$\left.- \frac{\widetilde{D}}{R}\frac{\boldsymbol{n}\times\boldsymbol{v}}{(1-\boldsymbol{v}\boldsymbol{n})^2}\right]_{t'} = \boldsymbol{n}\times\widetilde{\boldsymbol{E}}. \qquad (15)$$

These additional terms look like radiation terms; however, one cannot state that exactly because the change of the color charge vector does not result from a particle displacement and such a conclusion needs further special analysis. It is difficult also to compare directly these results with the Abelian case since the chromoelectric and chromomagnetic field strengths are not observable quantities. Accordingly, it is more consistent to consider the energy density of chromoelectric and chromomagnetic fields $\widetilde{E}^2/2$, $\widetilde{H}^2/2$ or the Wong force, which is analogous to the Lorentz force in electrodynamics [49] and serves as a measure for the momentum change of a color particle in an external color field. Such a role could also be played by a set of covariant functions, which define the strengths of chromoelectric and chromomagnetic fields at the different space-time points (in principle, one could determine the covariant gluon-parton distribution functions in the Weizsäcker-Williams ansatz).

In order to get well-settled approximate solutions we need further information that, e.g., can be obtained by solving the problem of two slowly moving color charges [50,51]. Assuming one particle to carry a color charge $\widetilde{P}$ and the other particle a charge $\widetilde{Q}$ we are allowed to simplify the consistency equations (10) for the pointlike sources to the following form:

$$\dot{\widetilde{P}} = g\widetilde{\varphi}(t,\boldsymbol{x}_1) \times \widetilde{P}, \quad \dot{\widetilde{Q}} = g\widetilde{\varphi}(t,\boldsymbol{x}_2) \times \widetilde{Q}, \qquad (16)$$

where the dot denotes the time derivative, $\boldsymbol{x}_1$ and $\boldsymbol{x}_2$ are the positions of the pointlike charges at time t, and $\widetilde{\varphi}(t,\boldsymbol{x}_i)$ is the value of the scalar potential at the charge location. An immediate consequence of Eqs. (16) is the conservation of the modulus of the particle color charge $\dot{\widetilde{P}}^2 = 0$ and $\dot{\widetilde{Q}}^2 = 0$. An analysis of the perturbation series in the coupling constant g and in particle velocity v/c shows that if the scalar potential $\widetilde{\varphi}$ is spanned by the two color vectors defined above

$$\widetilde{\varphi} = \varphi_1\widetilde{P} + \varphi_2\widetilde{Q}, \qquad (17)$$

(in particular, the first term of the iteration series looks similarly), then the vector potential $\widetilde{\boldsymbol{A}}$ (generated by the charges) is spanned by the vector product of charges only

$$\widetilde{\boldsymbol{A}} = \boldsymbol{a}\widetilde{P} \times \widetilde{Q}. \qquad (18)$$

In fact, Eqs. (17) and (18) fix the Coulomb gauge. Moreover, as a consequence of the vector algebra rules, contributions to the scalar potential are given only through the terms spanned by two charge vectors $\widetilde{P}$, $\widetilde{Q}$. Finally, the equation is factorized and we have the following system of equations for the potential components φ_1, φ_2 and the vector field $\boldsymbol{a}$

$$\boldsymbol{D}\boldsymbol{D}\Phi = \delta, \quad \nabla \times \nabla \times \boldsymbol{a} - g\boldsymbol{j} = 0, \quad \boldsymbol{j} = \Phi J\boldsymbol{D}\Phi, \qquad (19)$$

where the column $\Phi = \varphi - \overset{*}{\varphi}$ with $\varphi^T = \|\varphi_1,\varphi_2\|$, $\overset{*}{\varphi}^T = \|\overset{*}{\varphi}_1, \overset{*}{\varphi}_2\|$, $\overset{*}{\varphi}_1 = \varphi_1(\boldsymbol{x}_2)$, and $\overset{*}{\varphi}_2 = \varphi_2(\boldsymbol{x}_1)$ is the potential at the points of the charge location, $\delta^T = \|\delta(\boldsymbol{x}-\boldsymbol{x}_1), \delta(\boldsymbol{x}-\boldsymbol{x}_2)\|$, $\boldsymbol{D}_{kl} = \nabla\delta_{kl} + g\boldsymbol{a}C_{kl}$, $k,l = 1,2$ is the covariant

derivative, and C, J are the following matrices:

$$C = \left\| \begin{matrix} -(\widetilde{P}\widetilde{Q}) & -(\widetilde{Q}\widetilde{Q}) \\ (\widetilde{P}\widetilde{P}) & (\widetilde{P}\widetilde{Q}) \end{matrix} \right\|, \quad J = \left\| \begin{matrix} 0 & 1 \\ -1 & 0 \end{matrix} \right\|.$$

Here the parentheses denote the scalar product of charge vectors and δ is the δ-function source of unit intensity. Then Eqs. (16) achieve the following form :

$$\dot{\widetilde{P}} = g \overset{*}{\varphi}_2 \, \widetilde{Q} \times \widetilde{P}, \quad \dot{\widetilde{Q}} = g \overset{*}{\varphi}_1 \, \widetilde{P} \times \widetilde{Q}. \tag{20}$$

This system of Eqs. (20) describes the rotation of color charges with respect to the constant vector $\widetilde{\Omega} = \overset{*}{\varphi}_1 \, \widetilde{P} + \overset{*}{\varphi}_2 \, \widetilde{Q}$ with the frequency $g|\widetilde{\Omega}|$. The matrix C is conserved $dC/dt = 0$, so the potentials of the scalar φ and vector field $\boldsymbol{a}$ are quasistatic, indeed.

The set of Eqs. (19) has a transparent physical interpretation. The color field, generated by two pointlike sources, is the source of a color charge itself. Thus, a self-consistent environment of color charges and the corresponding currents is established in the space around the charges. The solutions of this system were investigated in detail both analytically and numerically in Ref. [51]. There, it was demonstrated that the interaction between color charges is Coulomb-like. If the coupling constant is not large, i.e., $g^2/(4\pi) < \sqrt{2}$, the corresponding solution can be well approximated by the Coulomb potentials $\varphi_{1,2} = 1/(4\pi|\boldsymbol{x} - \boldsymbol{x}_{1,2}|)$ with the vector field $\boldsymbol{a}$ that is generated by these potentials in the next iteration in g. This is illustrated in Fig. 1 by drawing the lines of constant force for $\boldsymbol{a}$ [see Fig. 1(a)] and equi-potentials for the induced chromomagnetic field $H_\varphi = \text{rot } \boldsymbol{a}$ [Fig. 1(b)], respectively. A line of force is a directed curve in the color field such that a forward tangent at any point shows the direction of the chromofield intensity. It is seen that the vector field of two color charges looks like the field of a permanent magnet with poles being placed at the points $\boldsymbol{x}_1, \boldsymbol{x}_2$. The vector field $\boldsymbol{a}$ develops a constant longitudinal component $|\boldsymbol{a}_\parallel| = 1/(4\pi|\boldsymbol{x}_1 - \boldsymbol{x}_2|)$ only along the straight line connecting the sources at $z_1 = 0$ and $z_2 = 1$, as demonstrated in Fig. 1, where the current lines of the vector field $\boldsymbol{a}$ are presented. The field drops sharply perpendicular to the line on which the color charges are located. The chromomagnetic field includes a single (vortex) component and, for example, for color charges at the points 0

and 1 on the axis z, is given by

$$\widetilde{H}_\varphi = \frac{g^3}{(4\pi)^2} \frac{1}{r} \left(\frac{1-\mu}{1+\mu} \right)^{1/2} \left(1 - \frac{1+r}{(1 - 2r\mu + r^2)^{1/2}} \right)$$
$$\times \widetilde{P} \times \widetilde{Q} \equiv H_\varphi \, \widetilde{P} \times \widetilde{Q}, \tag{21}$$

where r, μ are the spherical coordinates measured from the origin and $\mu = \cos\theta$ with the angle θ measured with respect to the z axis. The contour lines of the H_φ component of the chromomagnetic field are presented in Fig. 1(b). It is noteworthy that the lines of constant force and equipotentials seem to be mutually orthogonal at each z, r point. Equation (21) becomes more complicated for other choices of the charge location.

The total energy concentrated in the color field may be estimated as

$$\text{E} = \int d^3x \frac{\widetilde{\boldsymbol{E}}^2 + \widetilde{\boldsymbol{H}}^2}{2} \simeq \alpha_g \frac{(\widetilde{P}\widetilde{Q})}{|\boldsymbol{x}_1 - \boldsymbol{x}_2|} + \alpha_g^3 I \frac{(\widetilde{P} \times \widetilde{Q})^2}{|\boldsymbol{x}_1 - \boldsymbol{x}_2|}, \tag{22}$$

with $\alpha_g = g^2/(4\pi)$, $I = (6 - \pi^2/2)/4$; the terms of the source self-interaction are not included here. These estimates of the energy density of the chromomagnetic and chromoelectric fields clearly demonstrate the relative contributions of the first and subsequent iterations as well as the dominant role of the first iteration in the coupling constant relevant for actual applications in ultrarelativistic nucleus-nucleus collisions.

A closer analysis shows that the potentials φ_i have a singularity in the locations of the charges. The limiting values $\overset{*}{\varphi}_i$ [cf. Eqs. (20)] depend on the path by which one arrives at the charge position. For example, for one of the charges in the origin we get

$$\varphi_1 = -\frac{1}{4\pi} \frac{1}{|\boldsymbol{x}|} - \frac{g^3}{4\pi} a\mu(\widetilde{P}\widetilde{Q}) + \cdots$$

$$\varphi_2 = -\frac{1}{4\pi} \frac{1}{|\boldsymbol{x} - \boldsymbol{x}_2|} + \frac{g^3}{4\pi} a\mu(\widetilde{P}\widetilde{P}) + \cdots,$$

where a is the value of the longitudinal component of the vector field $\boldsymbol{a}_\parallel$ at the location point of the charge. Formally, the presence of singularities leads to a contradiction with
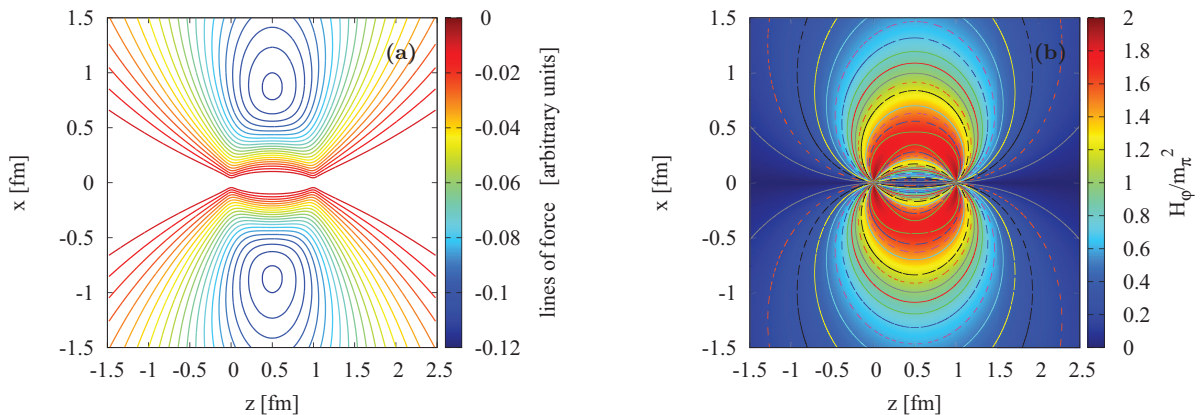

FIG. 1. (Color online) Schematic view of the lines of force of the vector field $\boldsymbol{a}$ (a) and the isolines of the chromomagnetic field component $H_\varphi = \text{rot } \boldsymbol{a}$ (b). The results are given for the cylindrical symmetry with two charges located at the points with $z = 0$ and 1.

the initial assumptions of deriving Eqs. (20) because now a mismatch of the color vector rotation on the charge itself is possible. In fact, it signals the necessity of a more accurate fixing of boundary conditions on the charge (this problem is akin to similar problems of diffraction theory). In particular, if these conditions are formulated in such a way that the vector field $\boldsymbol{a}$ does not penetrate into the sources, one can avoid these difficulties [52]. However, the approximate solutions are still quite appropriate to be used for the coupling constants, which are of interest for applications. Then it can be shown that the solutions of Eq. (19) with a boundary condition that leads to expelling the vector field from the charge should be qualitatively restructured when the coupling constant reaches the threshold values

$$\Pi = \frac{g^2}{(4\pi)^2}\widetilde{P}^2 \leqslant l(l+1), \qquad (23)$$

where $l = 0, 1, 2, \ldots$ are integers (of angular momentum) and $l = 0$ corresponds to the situation with the penetrating vector field. In addition to these critical values there is another one: it results from the same characteristic equation that we have used to obtain the limit (23) and is associated with the singularity power of (19) solutions in the neighborhood of the origin, where the source of the color charge $\widetilde{P}$ is located. Searching for the solution of $(\varphi_i - \overset{*}{\varphi}_i)$ and the vector field component a in the form of r^σ we obtain for the exponent σ

$$\sigma = -\frac{1}{2} \pm \frac{[(2l+1)^2 - 4\pi]^{1/2}}{2}.$$

The condition to treat only the real-valued solutions

$$\Pi \leqslant (l + 1/2)^2 \qquad (24)$$

leads to the constraint widely discussed some time ago [53]. It was asserted that when reaching this threshold the non-Abelian fields develop instability and, as a consequence, the color charge becomes completely screened. However, one can notice that the critical values (23) are always reached before the limit (24) becomes effective and, therefore, a rearrangement of the vector field takes place before the complete color charge screening develops. The proper time-consuming calculations are possible only by applying numerical schemes with the vanishing divergence. Fortunately, such effects occur for coupling constants, which apparently are of little interest for the applications.

The scalar component of Eqs. (19) can be written in the form

$$\nabla \boldsymbol{E} = \delta - \boldsymbol{a}C\boldsymbol{E},$$

where a column of two components of the chromoelectric field $\boldsymbol{E} = \boldsymbol{D}\Phi$ has been introduced. The last term includes the vector field $\boldsymbol{a}$ and can be interpreted as a charge density cloud (column of charges G_1, G_2) of the gluon field

$$G = -\boldsymbol{a}C\boldsymbol{E}.$$

Intuitively, it appears plausible that if the color sources are antiparallel, then the charge of the non-Abelian field could be zero. Indeed, if $\widetilde{P} = -\widetilde{Q}$, then by calculating the charge density components $G_1 = G_2 = \boldsymbol{a}\nabla(\Phi_2 - \Phi_1)$, it

becomes clear that the charge of the non-Abelian field indeed vanishes $\widetilde{G} = G_1\widetilde{P} + G_2\widetilde{Q} = 0$. In contrast, we expect that the non-Abelian field charge becomes maximal if the color charges of the particles are parallel $\widetilde{P} = \widetilde{Q}$. In this situation $G_1 = -G_2 = \boldsymbol{a}\nabla(\Phi_1 + \Phi_2)$, where, contrary to expectations, the non-Abelian field charge gets zero $\widetilde{G} = 0$ again. Note, however, that the charge of the non-Abelian field will be nontrivial for other configurations.

It is important to notice that the energy of the system of the non-Abelian field and the particles can be written [if based on the solutions of Eqs. (19)] in the following form:

$$E = \int d^3x \frac{\widetilde{E}^2 + \widetilde{H}^2}{2} = \frac{1}{2}\int d^3x(-\widetilde{\varphi}\widetilde{\delta} + \widetilde{\varphi}\widetilde{G}), \qquad (25)$$

where in accordance with Eq. (17) $\widetilde{\delta} = \delta_1\widetilde{P} + \delta_2\widetilde{Q}$, i.e., the chromomagnetic component effectively transforms into a charge. This form reminds us of the well-known expression of electrodynamics for the electrostatic energy of a system of charges

$$E = -\frac{1}{2}\sum_i \varphi_i e_i,$$

where φ_i is the potential (that can already be considered as an observable quantity) at the location point of the charge e_i. Comparing these expressions we are able to conclude clearly about the role of the non-Abelian charge cloud and, taking into account the sign of its contribution to the energy [see Eq. (22), for example] we find that extra repulsion is developed in the system of non-Abelian charges. We speculate that this extra repulsion might also lead to enhancement of the elliptic flow v_2 of hadrons in relativistic heavy-ion collisions, which has not been considered so far.

In view of the classical field dynamics we realize that Eq. (25) serves as the only source of information on the forces acting in the system. It is interesting to remark that, e.g., the Wong force (invented to describe the dynamics of color charges in an external field) is associated only with the first term $\sim \widetilde{\varphi}\widetilde{\delta}$ of Eq. (25), as it should be in the chromostatic case, since it is the only combination permitted to construct properly its covariant momentum extension. It can also be constructed by counting the Wong force for the first and second charge explicitly (using the definition of the chromoelectric field strength $\widetilde{E}$):

$$\boldsymbol{F}_P = \widetilde{P}\widetilde{\boldsymbol{E}}(\boldsymbol{x}_1) = \nabla\varphi_1|_{\boldsymbol{x}_1}\widetilde{P}^2 + \nabla\varphi_2|_{\boldsymbol{x}_1}(\widetilde{P}\widetilde{Q}),$$
$$\boldsymbol{F}_Q = \widetilde{Q}\widetilde{\boldsymbol{E}}(\boldsymbol{x}_2) = \nabla\varphi_1|_{\boldsymbol{x}_2}(\widetilde{P}\widetilde{Q}) + \nabla\varphi_2|_{\boldsymbol{x}_2}\widetilde{Q}^2.$$

Singular contributions describe self-interactions and should be regularized as in electrodynamics. Equation (25) demonstrates explicitly that the superposition principle for a color charge is nonapplicable in the general situation and one has to accurately account for the non-Abelian field cloud energy. The structure of the cloud environment and, hence, the system energy depends, generally speaking, on the choice of the boundary condition for the charge.

It is relevant to notice that the iterative perturbation series can be analyzed [when dealing with the Yang-Mills systems (9)] even when discarding the compatibility condition (10). The correct construction of the iterative series

inevitably leads to the conclusion about the nonconservation of classical color charge. This property is essentially different from naively expected small corrections to the Abelian solutions because of the nonlinearity of the Yang-Mills equations. In a sense this conclusion can be used in the inverse manner that the solutions are automatically correct with accuracy of an order of g [in reality g^3, see (25)] if the compatibility conditions are taken into account. In the non-Abelian case it is technically difficult to operate with the different gauges and besides, the set of physically justified (gauge invariant) observables is less than in electrodynamics.

Since the strengths of chromoelectric and chromomagnetic fields are not proper observables, the problem arises in interpreting their solutions. Actually, in the example discussed above the gauge is implicitly fixed by selecting a special type of solution. If one makes a choice in favor of the rest frame of the rotating charges, the potentials $\varphi_{1,2}$ approach some constants at spatial infinity. Such a gauge is inconvenient to be used in numerical calculations and our experience suggests that the Coulomb solutions are most informative.

Adding even one more color charge makes it impossible to investigate the problem at the same level of consistency as for the two-particle problem because the compatibility equations (10) cannot be integrated anymore. Nevertheless, it seems reasonable to consider that the system energy is given by the same expression (25) with the Coulomb interaction of the components. The charge contributions of non-Abelian fields (diffusive color clouds) are small for the coupling constants of actual interest because in the relativistic heavy-ion situation it is impossible to factorize the equations in a general form and the problem arises of how to construct an approximate solution.

IV. FIELD OF TWO COLOR CHARGES

Let us first consider the field of two color charges $\widetilde{P}$, $\widetilde{Q}$ moving along the z axis towards each other with velocities v and $-w$, respectively. If their encounter is supposed to take place at time $t = 0$, their coordinates in the laboratory system are given as $z_1 = vt, z_2 = -wt$. Obviously, when the particles are far from each other their interaction can be assumed weak and their charges remain constant with high accuracy.

Adapting the typical scale of non-Abelian (strong) interactions of about 1 fm we assume that the interaction is switched on just at this distance (scale) denoted by D. Obviously, this generates the characteristic time scale in the problem. Then the first milestone appears when the particles enter the interaction area, i.e.,

$$T = -\frac{D}{v + w}. \tag{26}$$

The second time instant of importance is t_1' when a signal of the appearance of charge $\widetilde{Q}_T$ at the distance of 1 fm reaches the first particle (with the color charge $\widetilde{P}$). Similarly for the second particle, the time when the charge $\widetilde{P}_T$ comes at the same distance is denoted by t_2', where $\widetilde{P}_T$, $\widetilde{Q}_T$ are the color charges before entering the zone of interaction, i.e., before the time T,

$$t_1' = \frac{1-w}{1+v}T, \quad t_2' = \frac{1-v}{1+w}T. \tag{27}$$
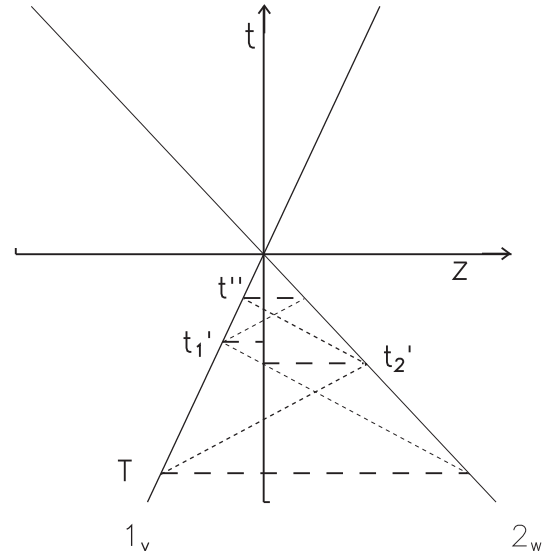

FIG. 2. The time scheme for the meeting of two color particles. The solid lines are the particle trajectories, the dashed lines show projections on the time axis, the dotted lines are the light signals. Here T is the initial time of the interaction when the particles become closer than the distance $D = 1$ fm; t_1' is the arrival time of the signal to the first particle about the presence of the color charge $\widetilde{Q}_T$ at 1 fm; similarly for the second particle; t_2' is the time when the charge $\widetilde{P}_T$ is seen at the same distance, where $\widetilde{P}_T$, $\widetilde{Q}_T$ are the charges before entering the interaction zone, i.e., before the time T. Until the time t'', the first and the second particles rotate with respect to constant color vectors $\widetilde{Q}_T$, $\widetilde{P}_T$.

These expressions are easily extracted from the scheme in Fig. 2 by writing out the relations for the arrival of the light signals and charges at the points of interest. In the figure, these events take the form of the corresponding triangles. Just at these times the color charges start to rotate with respect to their constant color vector, which is the vector peculiar to the partner charge before it entered the interaction area. This regime is going on up to the time

$$t'' = \frac{1-w}{1+v}\frac{1-v}{1+w}T, \tag{28}$$

which is the same for both particles. It is also the time necessary for a signal to reach the partner providing information on the beginning of rotation [see Eqs. (20)] starting from its asymptotic charge value $\widetilde{P}_T$, $(\widetilde{Q}_T)$. It is noteworthy that the same approach is used for formulating properly the Cauchy problem for retarded equations [54].

The velocity of a relativistic particle is determined by the relation

$$v = \left(1 - \frac{m^2}{\mathcal{E}^2}\right)^{1/2} \simeq 1 - \frac{m^2}{2\mathcal{E}^2}, \tag{29}$$

where m is the particle mass and $\mathcal{E}$ its energy. It allows us to estimate the order of magnitude for the characteristic time in the problem as

$$t' \sim \frac{m^2}{\mathcal{E}^2}T, \quad t'' \sim \frac{m^4}{\mathcal{E}^4}T.$$

The collision energies of present heavy-ions facilities (RHIC and LHC) allow us to estimate the corresponding factors as $\mathcal{E}/m \sim 10 - 10^2$ and more. In Secs. V and VI, where charge-dipole and dipole-dipole scattering is considered, another interesting scale arises. It is the distance δ between the dipole charges and we assume it to be of the order of the interquark distance in the nucleon, i.e., $\delta = 1$ fm. Then in the laboratory system the dipole size (due to Lorentz contraction) will be

$$\Delta = \delta(1 - v^2)^{1/2} \sim \delta \frac{m}{\mathcal{E}}.$$

Let us denote the time corresponding to this scale by $t_3 \sim m/\mathcal{E}$ (see below). Thus, for the relativistic problem of interest we obtain the following temporal hierarchy of interaction stages

$$t'' \ll t' \ll t_3 \ll T.$$

Due to the chosen geometry of the problem an approximate solution of the Yang-Mills equations for two color charges can be represented as the following superposition [see also (11)]:

$$\widetilde{\varphi} = [\varphi_1 \widetilde{P}]_{t'} + [\varphi_2 \widetilde{Q}]_{t'}, \quad \widetilde{A}_z = v[\varphi_1 \widetilde{P}]_{t'} - w[\varphi_2 \widetilde{Q}]_{t'}. \quad (30)$$

The scalar potentials φ_1 and φ_2 can be specified as:

$$\varphi_1 = \frac{1}{4\pi} \frac{g}{R_1 - vR_1}, \quad \varphi_2 = \frac{1}{4\pi} \frac{g}{R_2 - wR_2}. \quad (31)$$

The factor g is taken out since the normalization of the color charge vectors of the particles is chosen as unity. The consistency conditions (14) include the potentials at the location point of the particles. Let z_1 and z_2 be the coordinates of the particles at some moment (see Fig. 3). From this picture one can conclude that the potential values of interest are
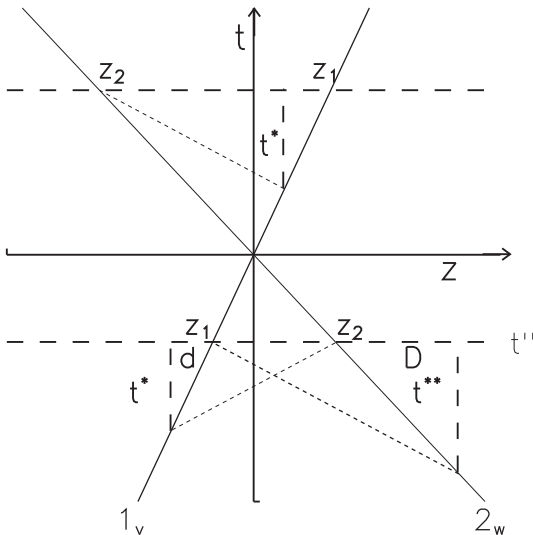

FIG. 3. The scheme for determining the retardation time for the collision of two charges. Here z_1 and z_2 are the current positions of the particles at two certain time moments. The charge of the first particle is characterized by the retarded time t^{**} as well as by a segment D which measures the distance between the particles for this time. The parameters t^* and d for the second particle have a similar meaning (see text).

determined by the distance

$$R_1 = d + z_2 - z_1 = t^*, \quad R_2 = D + z_2 - z_1 = t^{**}$$

with $d = vt^*$ and $D = wt^{**}$. Using these relations, we obtain

$$\varphi_1 = \frac{1}{4\pi} \frac{g}{z_2 - z_1}, \quad \varphi_2 = \frac{1}{4\pi} \frac{g}{z_2 - z_1}.$$

Thus, the Lorentz factors are compensated in such a way that the scalar potentials at the charge location can be simply expressed in terms of the distance between the particles in the current moment. Also, taking into account the form of the vector potential, we arrive at the following expression for the compatibility conditions:

$$\dot{\widetilde{P}} = \alpha_g \frac{1 + vw}{|z_1 - z_2|} \widetilde{Q}(t - t_{12}^{**}) \times \widetilde{P},$$
$$\dot{\widetilde{Q}} = \alpha_g \frac{1 + vw}{|z_1 - z_2|} \widetilde{P}(t - t_{21}^{*}) \times \widetilde{Q}. \quad (32)$$

The retarded time can be obtained (using Fig. 3, for example), as

$$t_{21}^{*} = -\frac{v + w}{1 - v}t, \quad t_{12}^{**} = -\frac{v + w}{1 - w}t, \quad \text{for} \quad t < 0.$$

For $t > 0$ (in the above formulas) the following replacement should be made: $v, w \to -v, -w$. In the electromagnetic case, the charge is conserved and its retarded time is defined simply as $t = t' + R(t')/c$ [43]. Below we will apply the reduced notation for the retarded time without any further explanation.

It is convenient to introduce an auxiliary variable $\chi = -\ln|t|$, by means of which Eqs. (32) are reduced to

$$\widetilde{P}' = \omega \widetilde{Q}(\chi - \Delta^*) \times \widetilde{P}, \quad (t < 0)$$
$$\widetilde{Q}' = \omega \widetilde{P}(\chi - \Delta^{**}) \times \widetilde{Q}, \quad (33)$$

for negative times, and

$$\widetilde{P}' = -\omega \widetilde{Q}(\chi + \Delta^{**}) \times \widetilde{P}, \quad (t > 0)$$
$$\widetilde{Q}' = -\omega \widetilde{P}(\chi + \Delta^*) \times \widetilde{Q}, \quad (34)$$

for positive times. Here the prime denotes differentiation with respect to χ,

$$\omega = \alpha_g \frac{1 + vw}{v + w}, \quad \Delta^* = \ln \frac{1 + v}{1 - w}, \quad \Delta^{**} = \ln \frac{1 + w}{1 - v}.$$

The procedure for obtaining an approximate solution is given in the Appendix. To find the strength of the chromo-electric and chromomagnetic fields, it is also required to know the derivatives of the color charge vectors with respect to the retarded time $d\widetilde{P}(t')/dt'$, $d\widetilde{Q}(t')/dt'$. They are computed by the explicit formulas (32).

As an example, let us consider the field created by two relativistic particles moving with velocities: $v = 1 - 2 \times 10^{-2}$ and $|w| = 1 - 1 \times 10^{-2}$. The energy-mass ratio for the first particle is $\mathcal{E}/m \simeq 16$, and for the second particle is $\mathcal{E}/m \simeq 22$. Let us take the coordinates of the observation point as $r_0 = (2, 0, 1)$, i.e., $x = 2$ fm and $z = 1$ fm. For comparison, we consider also the field created by particles with electric charge

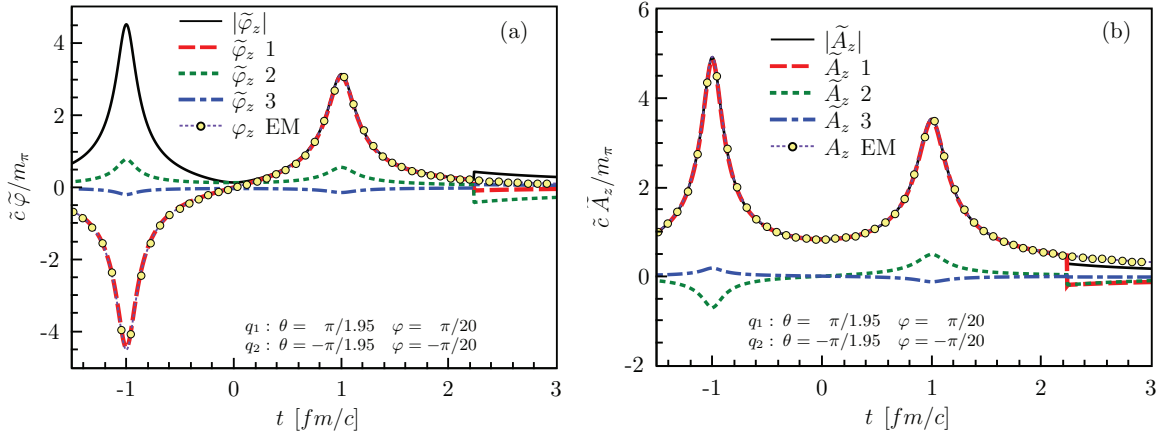FIG. 4. (Color online) Time evolution of three color components for the scalar $\widetilde{\phi}$ (a) and z component of the vector potential $\widetilde{A}_z$ (b) for two oppositely directed charges in color space as a function of time is given by the dashed lines. The solid line shows the absolute value of the isovector potential $|\widetilde{\phi}|$. The electrodynamic potential with charges $\pm e$ corresponding to the coupling constant $\alpha_e = 0.3$ is displayed by open circles.

$\pm e$ of the same interaction strength as the color charges $[e^2/(4\pi) = g^2/(4\pi) = 0.3]$ moving with the same velocities. The potentials for the scalar $\widetilde{\varphi}$ and z component of the vector $\widetilde{A}_z$ fields of color particles are presented in Fig. 4 where the initial angles in the color space are determined as $\theta = \pi/1.95$, $\phi = \pi/20$ for the first particle and $\theta = -\pi/1.95$, $\phi = -\pi/20$ for the second one. In this case the color charge of the first particle, for example, will be $\widetilde{P} = (P_1, P_2, P_3)$, with $P_1 = \sin\theta\cos\phi$, $P_2 = \sin\theta\sin\phi$, $P_3 = \cos\theta$. This configuration of color charges $\widetilde{P}, \widetilde{Q}$ corresponds to almost oppositely directed charges at the initial stage. The dashed lines in this figure show the three color components of the scalar potential [Fig. 4(a)] and the third component of the vector potential [Fig. 4(b)]. The open circles are plotted for the potentials corresponding to the enhanced electrodynamic coupling. The modulus of the scalar $|\widetilde{\varphi}|$ and vector $|\widetilde{A}_z|$ potential are displayed by the solid lines in Fig. 4. We recall again that these variables are not directly observable. The selected observation point $\mathbf{r}_0 = (2,0,1)$ introduces some asymmetry reminding us of the asymmetry in

the transverse plane for peripheral nucleus-nucleus collisions, which lead to some dominant component [43].

According to the choice of the geometry, we see that there are three maxima in the evolution of the chromofield, Fig. 5. The first maximum corresponds to the passage of the first particle at the closest distance to the observation point, then the second maximum corresponds to the passage of the second charge and a late third one for which there is no analogy in the electromagnetic field (the dotted line is flat in this time interval). The first two bumps are located symmetrically with respect to the meeting point $t = 0$. For the selected configuration of color charges, one of the components of the potentials, shown by the dashed lines, dominates and almost coincides with the appropriate modulus of vectors in the color space (solid line). The meeting point seen by an observer is located at a distance of $R = (x^2 + z^2)^{1/2} = \sqrt{5} \sim 2.24$ from $t = 0$. It is seen that there is a noticeable difference between the scalar and vector potentials as compared to the electrodynamic case (open circles) at the appropriate time. As discussed in the Appendix,
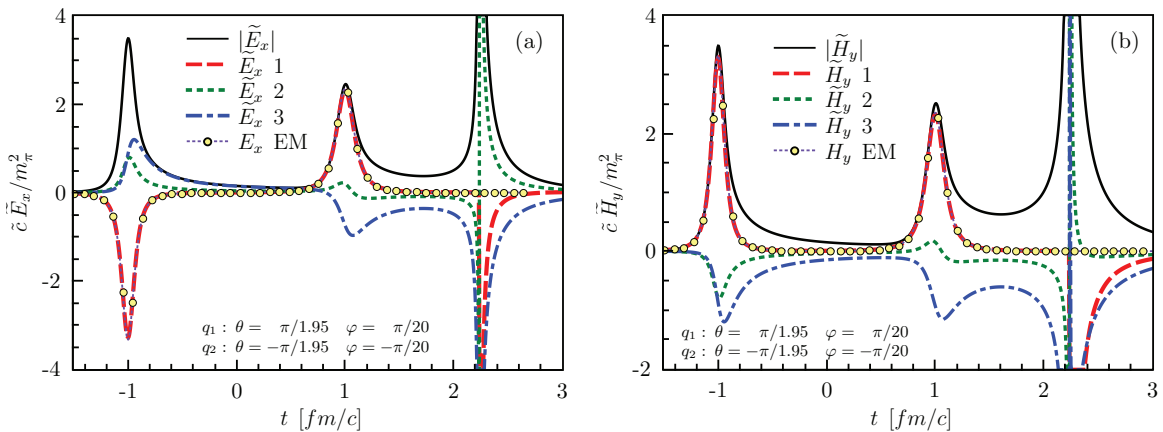

FIG. 5. (Color online) Three color components of the chromoelectric $\widetilde{E}$ (a) and chromomagnetic $\widetilde{H}$ field strength (b) for two moving color charges of opposite signs as a function of time are given by the dotted lines. The solid line shows the absolute value of the isovector potential $|\widetilde{E}|$. The open circles show the electrodynamic vector field corresponding to charges $\pm e$ and coupling constant $\alpha_e = 0.3$.
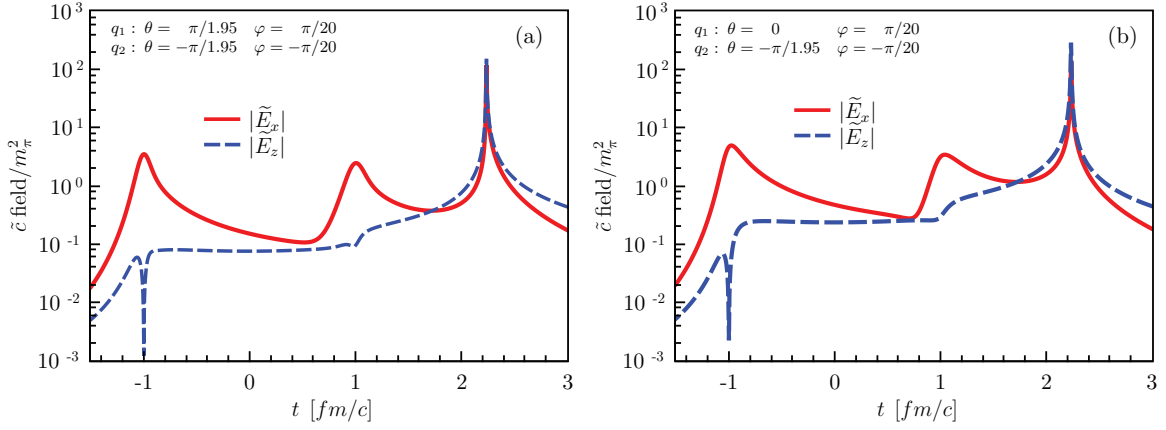
FIG. 6. (Color online) Modulus of the two components of the chromoelectric field strength $|\widetilde{E}_x|$ (solid line) and $|\widetilde{E}_z|$ (dashed line) for two moving charges with parallel (a) and orthogonal (b) color charges in the initial time.

the rotation of color charges is described by Eqs. (A1)–(A5). The effective rotation frequency in the neighborhood of the meeting point $t \to 0$ is $\omega'' = \alpha_q / \ln |t|$, i.e., the color charges are rotating infinitely fast near the meeting point.

The time dependence of the strength components of the chromoelectric $\widetilde{E}_x$ [Fig. 5(a)] and chromomagnetic $\widetilde{H}_y$ [Fig. 5(b)] fields is shown in Fig. 5 by the three dashed lines; the solid lines correspond to the modulus of the chromofields $|\widetilde{E}_x|$ and $|\widetilde{H}_y|$. We have cut the singular peaks at some threshold and thus the lines look somewhat irregular. In full agreement with Eqs. (15), the E_x and H_y components are dominating. In both cases two maxima (minima)—caused by passing the color charges in the vicinity of the observation point—are clearly visible. Note that here (and in what follows) the color field strength is plotted in dimensionless units where $\widetilde{c}$ is the color charge of the appropriate field component and m_π is the pion mass. The charge velocities considered roughly correspond to the RHIC energy where the maximal electromagnetic field eH_y/m_π^2 reaches a few units [43]. This value is essentially smaller than those in the color charge case (see Fig. 5). It is seen that for the color charge configuration considered the chromoelectric and chromomagnetic field are quite similar to the field in the case of enhanced ($\alpha_e = 0.3$) electrodynamics. Some differences in the height of the first two maxima are caused by different velocities of color charges. A significant difference at the third maximum is due to the arrival of a signal from the meeting point of particles to the observation point, where there is a noticeable additional contribution of chromoelectric and chromomagnetic fields associated with the temporal change of the particle color charges. This extra enhancement may be considered as a manifestation of the color vector rotation in the evolution of the color field strength named as the effect of the color charge glow. The color glow effect is not an artifact of the approximation but results from the pure non-Abelian term proportional to $\widetilde{D}$ in Eq. (15) as a distinct color wave disturbance arising due to the finite retardation time.

The modulus of the transverse $|\widetilde{E}_x| = \sqrt{\widetilde{E}_x^2}$ and longitudinal $|\widetilde{E}_z| = \sqrt{\widetilde{E}_z^2}$ component of the chromoelectric field is shown in Fig. 6 for two configurations of the initial color charges. The longitudinal component is strongly suppressed,

as it should be due to relativistic effects, but the signal from the meeting point of the particles leads to almost equal contributions. It is noteworthy that the change of the initial configuration of color charges from parallel to orthogonal [cf. Figs. 6(a) and 6(b)] does not change the evolution in the absolute values of the chromoelectric field though the signs of the color E_x, E_z components are different and change with time. It is also important to note that every collision noticeably changes the position of color charges in the color space but we do not present these scattering data here.

Characteristics for the initially almost orthogonal color charge vectors are presented in detail in Figs. 7 and 8. These results are obtained for particles with color charges defined by the following angles in color space: $\theta = 0$, $\phi = \pi/20$ for the first particle $\theta = -\pi/1.95$, $\phi = -\pi/20$ for the second one. We shall henceforth refer to this case as non-Abelian. The notation in these figures is identical to that in Figs. 4 and 5. The main result here is that in this case there is no dominant component, as in the case of mutually opposite charges considered above, but two preferred directions in color space are significant, as evidenced by the corresponding maxima shown by the dashed lines in Figs. 7 and 8. The third bump at $t = 2.24$ is again the manifestation of the color charge glow effect.

Some comments with respect to previous studies, addressing the color rotation in the encounters of color charges, are in order: In Ref. [55] the authors have solved the classical QCD equations of motion in perturbation theory up to order g^3 within light-cone variables (using the Mueller gauge transformation [56]) and assuming that the color charges move with the speed of light ($v = 1$) and the color interaction is switched on at $T = -\infty$. Their focus has been on the computation of soft gluons in the initial phase of ultrarelativistic nucleus-nucleus collisions in the forward light cone, in particular the gluon number, the gluon energy, and their multiplicity distributions. Though the basic equations (9) and (10) are the same, our model considers charges moving with velocities $v < 1$, subdivides the scattering process at three different stages (see Appendix) and takes into account the finite retardation time at each stage. As demonstrated above in Figs. 5 and 7, we are interested explicitly in the evolution of chromoelectric and chromomagnetic fields where
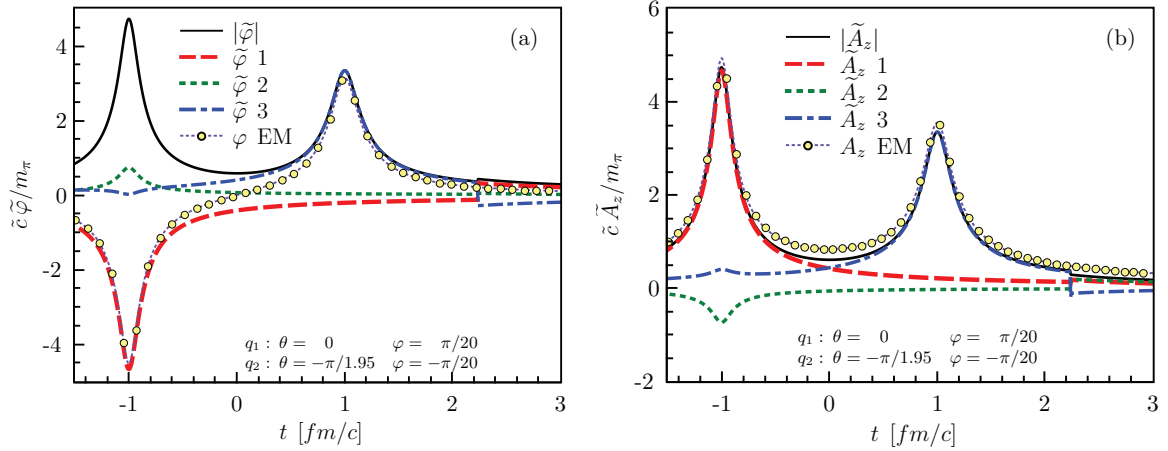
FIG. 7. (Color online) Non-Abelian configuration of color charges (see text). The three components of $\widetilde{\phi}$ (a) and $\widetilde{A}_z$ (b) are shown for the initially orthogonal charge vectors. The notation is the same as in Fig. 4.

the new color glow effect is observed most clearly. Since the authors of Ref. [55] compute the gluon field obtained by the Weizsäcker-Williams transformation of the potential and consider only global properties such as energy, number, and multiplicity distributions of gluons, a possible contribution of the color charge glow is hard to discriminate.

Furthermore, the space-time evolution of the classical gluon fields was investigated before in Ref. [57] within a rather similar non-Abelian model. This model, applied to the collision of two nuclei, exhibits a very complicated field structure associated with instabilities. In this picture, it is hardly possible to disentangle such a particular mode as the late effect of the color glow, which in principle could have left its traces also in their calculations. However, an additional investigation for simple colliding systems, as performed here, is mandatory to clearly pin down this phenomenon.

V. FIELD OF A COLOR CHARGE AND A COLOR DIPOLE

As in the previous section, let us assume that there is a particle with color charge $\widetilde{P}$ that moves along the z axis with velocity v. We denote it as the first particle. Suppose that the

dipole made up by the second and third particle with charges $\widetilde{Q}_2$ and $\widetilde{Q}_3$ is aligned along the z axis and moves in the opposite direction with velocity w. We denote the distance between the charges in the dipole as δ_w in its rest frame, which is taken as 1 fm. In the laboratory frame the charges are located closer to each other $\Delta'_w = (1 - w^2)^{1/2}\delta_w$ due to the Lorentz contraction. Let the first and second particle encounter at zero time before the time $t_3 = \frac{\delta'_w}{v+w}$ of the second meeting between the first and third particle (see Fig. 9). Then the trajectories of the first, second, and third charges are defined as $z_1 = vt$, $z_2 = -wt$, $z_3 = -wt + \delta'_w$. Similarly to Eq. (30), let us adopt an approximate solution of the Yang-Mills equations in the form

$$\widetilde{\varphi} = [\varphi_1 \widetilde{P}]_{t'} + [\varphi_2 \widetilde{Q}_2]_{t'} + [\varphi_3 \widetilde{Q}_3]_{t'},$$
$$\widetilde{A}_z = v[\varphi_1 \widetilde{P}]_{t'} - w[\varphi_2 \widetilde{Q}_2]_{t'} - w[\varphi_3 \widetilde{Q}_3]_{t'}. \tag{35}$$

The potentials at the location point of charges can be found in the same way as in the case of two color charges; this leads to the compatibility conditions for each of the charges, see
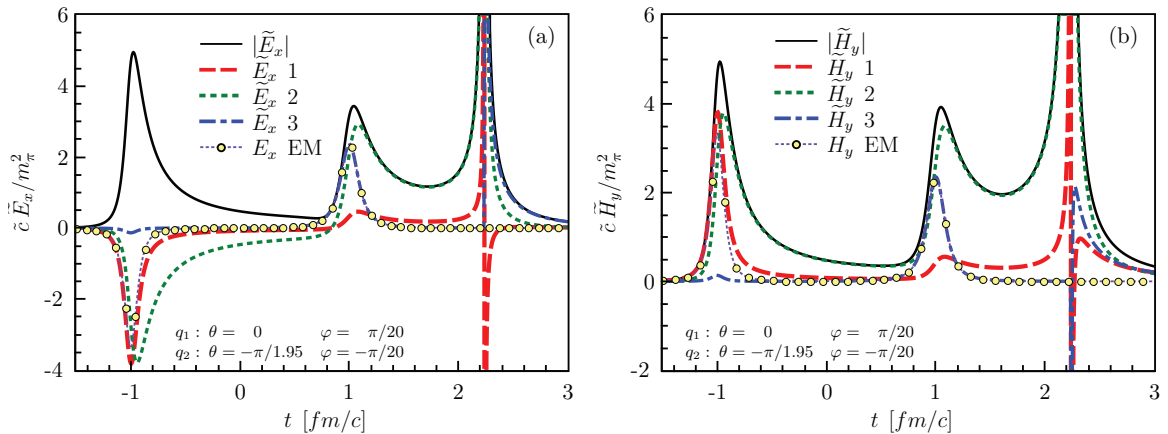

FIG. 8. (Color online) Non-Abelian configuration of color charges (see text). The three components of chromoelectric $\widetilde{E}$ (a) and chromomagnetic $\widetilde{H}$ (b) fields are shown for the initially orthogonal charge vectors. The notation is the same as in Fig. 5.
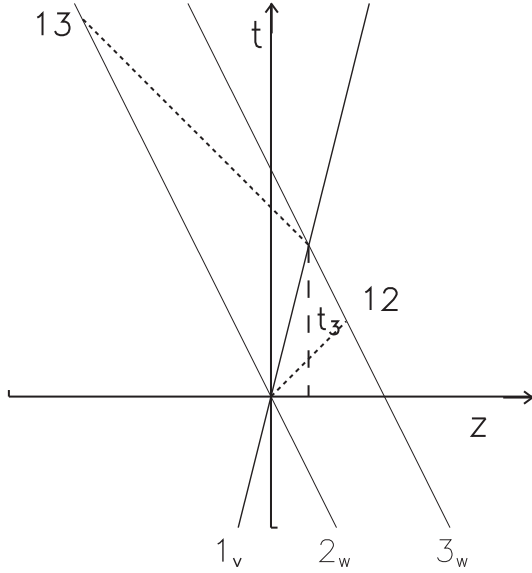
FIG. 9. Scheme of the meeting of a color particle and a dipole. The particle trajectories are plotted by the solid lines, the dotted lines are light-cone lines corresponding to the arrival of the signal from the particle meeting point. The arrival of the signal is marked by the points 12 and 13 (see text). The time t_3 is the moment when the first and the third particle meet each other.

Eq. (14)

$$\dot{\widetilde{P}} = \alpha_g \frac{1+vw}{|z_1 - z_2|} \widetilde{Q}_2(t - t_{12}^{**}) \times \widetilde{P} + \alpha_g \frac{1+vw}{|z_1 - z_3|}$$
$$\times \widetilde{Q}_3(t - t_{13}^{***}) \times \widetilde{P},$$

$$\dot{\widetilde{Q}}_2 = \alpha_g \frac{1+vw}{|z_1 - z_2|} \widetilde{P}(t - t_{21}^{*}) \times \widetilde{Q}_2 + \alpha_g \frac{1-w^2}{|z_2 - z_3|}$$
$$\times \widetilde{Q}_3(t - t_{23}^{***}) \times \widetilde{Q}_2,$$

$$\dot{\widetilde{Q}}_3 = \alpha_g \frac{1+vw}{|z_1 - z_3|} \widetilde{P}(t - t_{31}^{*}) \times \widetilde{Q}_3 + \alpha_g \frac{1-w^2}{|z_2 - z_3|}$$
$$\times \widetilde{Q}_2(t - t_{32}^{**}) \times \widetilde{Q}_3, \qquad (36)$$
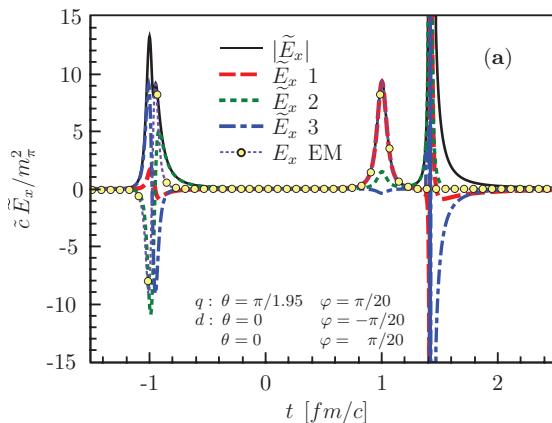
with $t_{31}^{*} = -\frac{v+w}{1+v}(t - t_3)$, $t_{13}^{***} = -\frac{v+w}{1+w}(t - t_3)$ for $t_3 < t$, and $t_{32}^{**} = \frac{v+w}{1+w}t_3$, $t_{23}^{***} = \frac{v+w}{1-w}t_3$ for $t < t_3$ (with the substitution $v, w \rightarrow -v, -w$). The retardation times are determined similarly to the case of two color charges, where, in particular, the retarded times t_{21}^{*} and t_{12}^{**} are given (see the relevant scheme in Fig. 3). An interesting peculiarity of the resulting system of Eqs. (36) is strong suppression of the contributions of charges 2 and 3 flying in the same direction, which enter into the equation with the Lorentz factor $1 - w^2$. Thus, in the ultrarelativistic case the mutual influence of color charges flying in the same direction may be ignored and the system can be considered as frozen. This is true even in the cases where the system has the size of a nucleus.

We are interested now in the particular case when the color dipole charges in the initial state are opposite, i.e., $\widetilde{Q}_3 = -\widetilde{Q}_2$. The prescription for obtaining an approximate solution in this case is given in the Appendix.

The strength of the chromoelectric and chromomagnetic fields—generated by particles moving with the velocity $v = 1 - 2 \times 10^{-2}$ and by the dipole with the velocity $|w| = 1 - 1 \times 10^{-2}$—is demonstrated in Fig. 10. The color charges of the particles at the initial time are determined by the following angles in the color space: $\theta = \pi/1.95$, $\phi = \pi/20$ for the first particle, $\theta = 0$, $\phi = -\pi/20$ for the second one and with the opposite angles for the third particle. This configuration is denoted as non-Abelian. We do not show explicit data for the potentials, as they provide little information. It is seen that generally the two first maxima of the field strength generated by color charges in the vicinity of the observation point are reasonably reproduced by the Coulomb-like solution (dotted lines in Fig. 10). However, the first maximum formed in passing the dipole is not smooth but has an up-down jump (or zigzag) shape. This structure is caused by the opposite color charges forming the dipole.

The observation point is located now in another place $x = 1$, $z = 1$ fm as compared to the case of the meeting of two particles at $x = 2$, so the signal of the meeting of the color charge and the dipole arrives at a time about $\tau = (x^2 + z^2)^{1/2}/c = \sqrt{2} \sim 1.41$. Here, at the meeting point the Coulomb-like solution predicts noticeably narrower distributions over the color field strength due to the so-called color
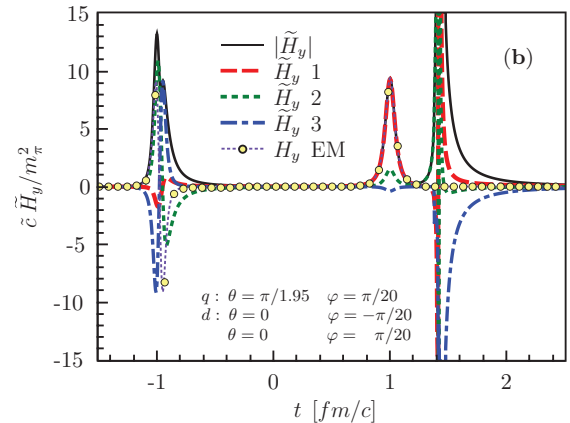

FIG. 10. (Color online) Chromoelectric $\widetilde{E}$ (a) and chromomagnetic $\widetilde{H}_y$ (b) fields for the charge-dipole case. The notation is the same as in Fig. 5.
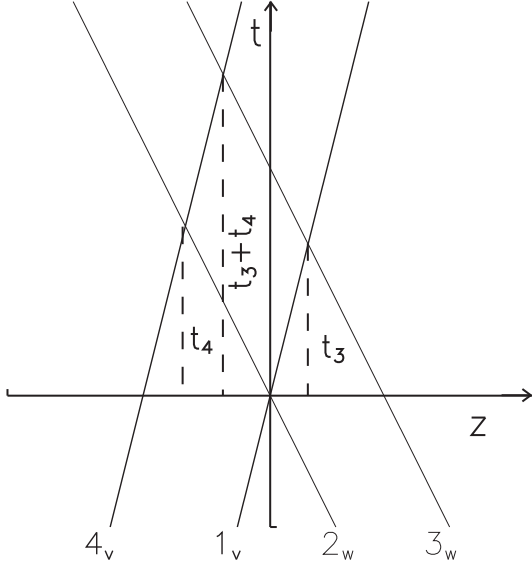
FIG. 11. Scheme of the meetings of two color dipoles. The solid lines are the particle trajectories. The meeting points of the particles are marked by t_3 for the particles 1-3, t_4 for the particles 4-2 and $t_3 + t_4$ for the particles 4-3.

charge glow, which, as noted above, results from the color charge interaction through the time dependence of the color vectors $\widetilde{D}$ [the last term in Eqs. (15)].

VI. FIELD OF TWO COLOR DIPOLES

Let us finally consider the field created by two color dipoles. The first dipole is formed by the first and fourth particle with charges $\widetilde{P}_1$ and $\widetilde{P}_4$, respectively. The second dipole is made up of the second and third particle with charges $\widetilde{Q}_2$ and $\widetilde{Q}_3$. At the initial time the color charge of each dipole is neutral: $\widetilde{P}_1 = -\widetilde{P}_4$, $\widetilde{Q}_2 = -\widetilde{Q}_3$. Particles of the first aligned dipole move along the z axis with velocity v and the second aligned dipole moves towards them with velocity w. Let us denote the distance between the charges in the first and second dipole in their rest system as δ_v and δ_w, respectively. In the laboratory frame, these distances are contracted $\delta'_v = (1 - v^2)^{1/2}\delta_v$ and

$\delta'_w = (1 - w^2)^{1/2}\delta_w$. Again, it is convenient to introduce the time scales

$$t_3 = \frac{\delta'_w}{v + w}, \quad t_4 = \frac{\delta'_v}{v + w},$$

when the first particle meets the third one and the fourth meets the second one, respectively (see Fig. 11). At the time $t_3 + t_4$ the fourth particle meets the third one. Suppose for convenience that the meeting of the first and second particle occurs at time zero. Then the trajectories of charges with numbers one, two, three, and four are defined as $z_1 = vt$, $z_2 = -wt$, $z_3 = -wt + \delta'_w$, $z_4 = vt - \delta'_v$. In this case the ansatz for the superposition of approximate solutions has the form

$$\widetilde{\varphi} = [\varphi_1 \widetilde{P}_1]_{t'} + [\varphi_2 \widetilde{Q}_2]_{t'} + [\varphi_3 \widetilde{Q}_3]_{t'} + [\varphi_4 \widetilde{P}_4]_{t'},$$

$$\widetilde{A}_z = v[\varphi_1 \widetilde{P}_1]_{t'} - w[\varphi_2 \widetilde{Q}_2]_{t'} - w[\varphi_3 \widetilde{Q}_3]_{t'} + v[\varphi_4 \widetilde{P}_4]_{t'}.$$
(37)

Similarly to the previous sections the compatibility condition [see Eq. (14)] for each charge can be written as follows:

$$\dot{\widetilde{P}}_1 = \alpha_g \frac{1 + vw}{|z_1 - z_2|} \widetilde{Q}_2(t - t_{12}^{**}) \times \widetilde{P}_1 + \alpha_g \frac{1 + vw}{|z_1 - z_3|}$$

$$\times \widetilde{Q}_3(t - t_{13}^{***}) \times \widetilde{P}_1 + \alpha_g \frac{1 - v^2}{|z_1 - z_4|} \widetilde{P}_4(t - t_{14}^{IV}) \times \widetilde{P}_1,$$

$$\dot{\widetilde{Q}}_2 = \alpha_g \frac{1 + vw}{|z_1 - z_2|} \widetilde{P}_1(t - t_{21}^{*}) \times \widetilde{Q}_2 + \alpha_g \frac{1 - w^2}{|z_2 - z_3|}$$

$$\times \widetilde{Q}_3(t - t_{23}^{***}) \times \widetilde{Q}_2 + \alpha_g \frac{1 + vw}{|z_2 - z_4|} \widetilde{P}_4(t - t_{24}^{IV}) \times \widetilde{Q}_2,$$

$$\dot{\widetilde{Q}}_3 = \alpha_g \frac{1 + vw}{|z_1 - z_3|} \widetilde{P}_1(t - t_{31}^{*}) \times \widetilde{Q}_3 + \alpha_g \frac{1 - w^2}{|z_2 - z_3|}$$

$$\times \widetilde{Q}_2(t - t_{32}^{**}) \times \widetilde{Q}_3 + \alpha_g \frac{1 + vw}{|z_3 - z_4|} \widetilde{P}_4(t - t_{34}^{IV}) \times \widetilde{Q}_3,$$

$$\dot{\widetilde{P}}_4 = \alpha_g \frac{1 - v^2}{|z_1 - z_4|} \widetilde{P}_1(t - t_{41}^{*}) \times \widetilde{P}_4 + \alpha_g \frac{1 + vw}{|z_4 - z_2|}$$

$$\times \widetilde{Q}_2(t - t_{42}^{**}) \times \widetilde{P}_4 + \alpha_g \frac{1 + vw}{|z_3 - z_4|} \widetilde{Q}_3(t - t_{43}^{***}) \times \widetilde{P}_4,$$
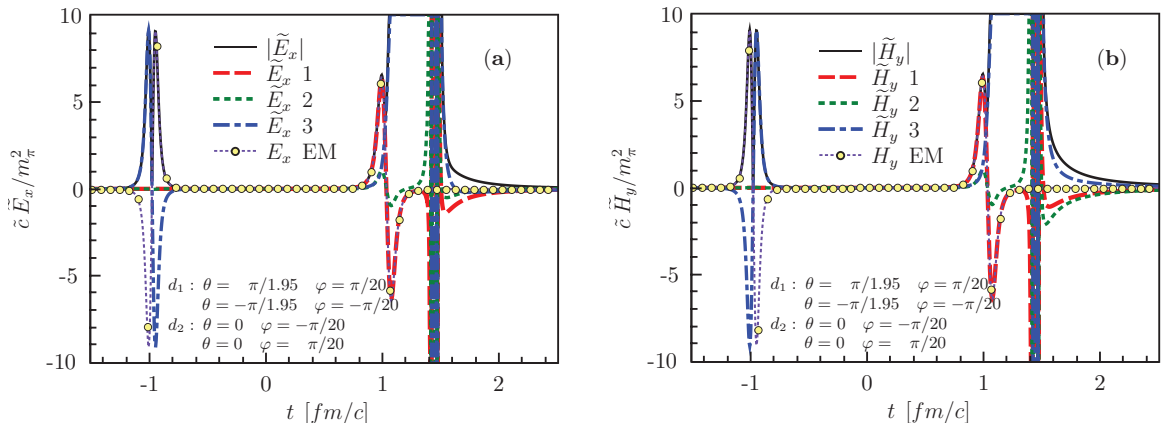(38)

FIG. 12. (Color online) The three components of $\widetilde{E}_x$ (a) and $\widetilde{H}_y$ (b) for the dipole-dipole case. The notation is similar to Fig. 5.
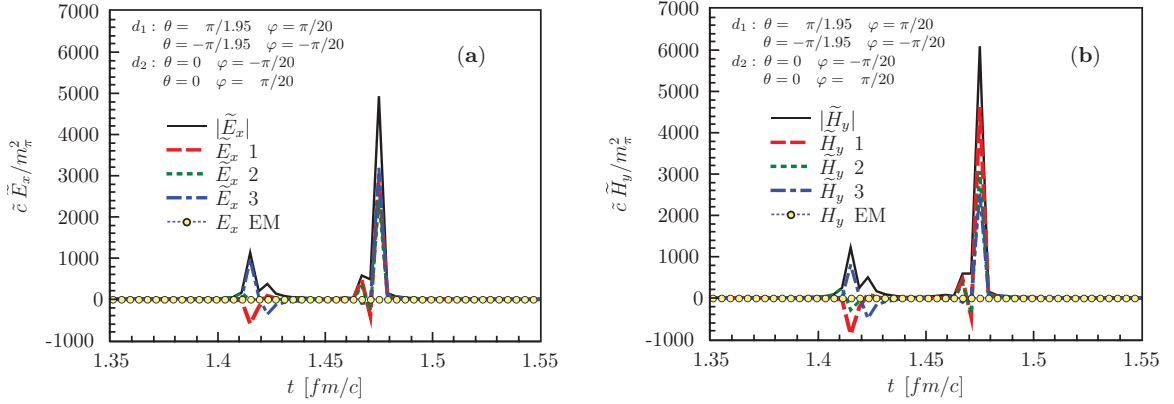
FIG. 13. (Color online) The same as in Fig. 12 but for the zoomed region near the meeting point.

where the different times are defined as $t_{42}^{**} = -\frac{v+w}{1-w}(t - t_4)$, $t_{24}^{IV} = -\frac{v+w}{1-v}(t - t_4)$ for $t < t_4$ (for $t_4 < t$, the substitution should be made $v, w \to -v, -w$); $t_{43}^{***} = -\frac{v+w}{1-w}(t - t_3 - t_4)$, $t_{34}^{IV} = -\frac{v+w}{1-w}(t - t_3 - t_4)$ for $t < t_3 + t_4$ (for $t_3 + t_4 < t$, the substitution should be made $v, w \to -v, -w$); $t_{41}^* = -\frac{v+w}{1-v}t_4$; and $t_{14}^{IV} = -\frac{v+w}{1+v}t_4$. In the Appendix we present the procedure for obtaining an approximate solution for two color dipoles.

In Fig. 12, the strength of chromoelectric and chromomagnetic fields created by two dipoles with the velocities $v = 1 - 2 \times 10^{-2}$ and $|w| = 1 - 1 \times 10^{-2}$ is demonstrated. The color charges of the particles at the initial time are determined by the following angles in the color space: $\theta = \pi/1.95, \phi = \pi/20$ for the first particle and $\theta = 0, \phi = -\pi/20$ for the second one and with the opposite angles for the third and fourth particle. As is seen (by the dotted lines in Fig. 12), the two first maxima are reproduced by the Coulomb-like solution including the up-down jump effect for both maxima, noted above in Sec. V. The observation point has the coordinates $x = 1$ fm and $z = 1$ fm, so the signal on the meeting of the color dipoles arrives at the time about $\tau = (x^2 + z^2)^{1/2}/c = \sqrt{2} \sim 1.41$. In fact, the whole area from the second maximum until the meeting point is filled by the chromoelectric and chromomagnetic fields of noticeable strength and near $\tau = 1.41$ this looks like a band. To clarify the band structure, we zoom into the region near the meeting point in Fig. 13. It is seen that this area consists of four maxima of huge intensity, which in dynamical systems can result in large local color fluctuations. This shining of the color charge glow is mainly due to color charge interactions through the time dependence of the color vectors $\tilde{D}$ [the last term in Eqs. (15)], which is certainly not reproduced by the Coulomb solution with the enhanced coupling. It is noteworthy that the color charge glow effect is getting even larger for more complicated systems.

VII. CONCLUSIONS

In this study, we have considered several elementary configurations of relativistic partons with non-Abelian charges for the SU(2) group in the classical limit. It is shown that, as in the case of nonrelativistic particles, the system generally shows Coulomb-like features, and the analogy is convincingly supported by a comparison with electrodynamics for the same coupling strength. In distinction, we find an additional strength of chromoelectric and chromomagnetic fields close to the meeting of particles, which is caused by the explicit time dependence of the color charge vectors. In the chosen gauge the interaction of the color charges results in the rotation of the color vectors, which becomes very fast close to the meeting point of two particles. The chromofields are stronger by about an order of magnitude than the corresponding electromagnetic fields created by a moving source at similar conditions. The longitudinal and transverse field components of this signal are of the same order of magnitude in contrast to the longitudinally compressed field (due to the Lorentz contraction). Changing the observation point one can see the predicted shift of the meeting signal of the particles. It turns out that for complex systems the whole observation zone—of the order of a few fm near the meeting point—is filled up by this intensive signal of a strong interaction scale, which we have denoted as color charge glow.

We emphasize that the new color charge glow effect, which was not identified explicitly in similar studies in the past [57], is a manifestation of the nonlinear nature of non-Abelian field dynamics and intimately related to the color vector rotation, which results in additional field strength from the previous encounter of color charges moving with velocity $v < 1$. This effect essentially becomes visible in the chromofield strength and may be not observed in global time-integrated observables such as the gluon energy and multiplicity distributions. In this respect, the effect of color charge glow is as robust as the color rotation itself.

In fact, there is no direct evidence of the Coulomb law for the interaction between quarks. The leading hypothesis to explain the observed behavior of quarks is the idea of vacuum gluon fields or gluon-field fluctuations. Our considerations do not provide an alternative to the CGC description of the very initial phase of ultrarelativistic nucleus-nucleus or proton-nucleus collisions but should be important at the later stage of the glasma evolution—when the CGC is melting and converting to a QGP with a considerable amount of quarks and antiquarks—as well as for the dynamics of hadronization at the late stage of the QGP evolution. In this paper, we have not touched upon these topics, but one should note that estimates

based on the instanton vacuum model indicate that the vacuum field may be much stronger than the fields generated by the collision of quarks [58]. Every open color in the instanton medium is screened, which indicates the impossibility of forming gluon fields of noticeable intensity and, in a physical sense, apparently implies the transformation of the gluon field quanta in energetically more favorable configurations.

With respect to our discussion of the energy of a non-Abelian system [see Eq. (25)], we speculate that the signals of the additional repulsive non-Abelian interaction might leave its traces in the early development of the collective flow in relativistic nucleus-nucleus collisions prior to partonic equilibrium.

Using the proposed approximation that particles begin to feel the presence of the non-Abelian charge of a collision partner only below the distance of 1 fm, the discussed color configurations can apparently be considered as a model for a color pre-quark/gluon matter. As to a possible formation of some objects, such as a color-flux tube, a larger system similar to that formed in ultrarelativistic heavy-ion collisions might be considered. Here new collective effects like the Debye screening come into play, additionally. However, these effects are beyond the aim of our study and are the subject of future investigations. Also, an important practical conclusion is that, in essence, the correct assessment for the strengths of chromoelectric and chromomagnetic fields is obtained just in the approximation of pure electrodynamics with enhanced coupling g^0. At the same time, the experience gained so far [59] indicates that such a signal of color charge glow might manifest itself not so directly as suggested by the figures above. Subsequent parton-parton collisions in dense matter—as produced in ultrarelativistic Pb + Pb (or Au + Au) collisions—may wash out this effect. Accordingly, the study of collisions of light nuclei or proton-nucleus interactions appears more promising.

APPENDIX

1. Time hierarchy of interaction stages

In the discussion of a color charge, a color dipole, and two dipoles we need to compare the description at different scales. It is convenient to specify them by the following items.

(i) The time $t < T$, $T \leqslant t < t''$ (recall $t'' < 0$). The form of the solution for negative times has already been specified above, for example, the color charge vectors are constant up to the scale t'

$$\widetilde{P} = \widetilde{P}_T, \quad t < t_1' \quad \widetilde{Q} = \widetilde{Q}_T, \quad t < t_2'. \quad \text{(A1)}$$

Further, up to the time t'', each charge rotates relative to the constant vector of the opposite charge particle. Let us introduce the basis (static) vectors in the color (isotopic) space, in terms of which it will be convenient to express the solutions of equations.

The triple orthogonal unit vectors are associated with the vector $\widetilde{P}$ in the form:

$$\widetilde{Q}_T, \quad \widetilde{n}_{P_T} = \frac{\widetilde{P}_T \times \widetilde{Q}_T}{\sin\theta}, \quad \widetilde{m}_{P_T} = \widetilde{Q}_T \times \widetilde{n}_{P_T},$$

where $\cos\theta = (\widetilde{P}_T \widetilde{Q}_T)$. A similar basis associated with the vector $\widetilde{Q}$ is defined as

$$\widetilde{P}_T, \quad \widetilde{n}_{Q_T} = -\widetilde{n}_{P_T}, \quad \widetilde{m}_{Q_T} = \widetilde{P}_T \times \widetilde{n}_{Q_T}.$$

The solution of Eqs. (32) for the times considered (A1) can be represented as follows:

$$
\begin{aligned}
\widetilde{P}_< &= \cos\theta\, \widetilde{Q}_T + \sin\theta \big\{ \cos[\omega(\chi - \chi_1')]\widetilde{m}_{P_T} \\
&\quad - \sin[\omega(\chi - \chi_1')]\widetilde{n}_{P_T} \big\}, \quad t_1' \leqslant t < t'', \\
\widetilde{Q}_< &= \cos\theta\, \widetilde{P}_T + \sin\theta \big\{ \cos[\omega(\chi - \chi_2')]\widetilde{m}_{Q_T} \\
&\quad - \sin[\omega(\chi - \chi_2')]\widetilde{n}_{Q_T} \big\}, \quad t_2' \leqslant t < t'',
\end{aligned}
\quad \text{(A2)}
$$

where we use the notation $\chi_1' = -\ln|t_1'|$, $\chi_2' = -\ln|t_2'|$.

(ii) The time $t'' \leqslant t \leqslant -t''$. Now consider the asymptotic solutions for large χ (in the neighborhood of the meeting point of particles). In this case, one can neglect the retardation factors Δ^*, Δ^{**} in Eqs. (33) and (34). Then, for both positive and negative times these equations describe the rotation of the color charge vector with respect to the vector $\widetilde{P} + \widetilde{Q}$, which is conserved. It seems reasonable to approximate the solutions of Eqs. (32) on the whole semiaxis of the negative time including the time of the meeting of particles, by matching the solutions on the t' scale with those on the t'' scale, where the retardation is neglected. The numerical study of the system (32) justifies in general such an approximation. Thus, at the time t'' the color vectors are

$$\widetilde{P}'' = \widetilde{P}_<(t''), \quad \widetilde{Q}'' = \widetilde{Q}_<(t'').$$

Therefore, the vector $\widetilde{P} + \widetilde{Q}$ is defined with respect to which vector of the color charge particles is rotated on the scale $T'' < t < 0$. Similarly to the considered case of solutions for large time t', let us introduce three orthogonal unit vectors

$$
\widetilde{\Omega} = \frac{\widetilde{P}'' + \widetilde{Q}''}{|\widetilde{P}'' + \widetilde{Q}''|}, \quad \widetilde{n}_{P''} \frac{\widetilde{P}'' \times \widetilde{\Omega}}{|\widetilde{P}'' \times \widetilde{\Omega}|},
$$
$$
\widetilde{m}_{P''} = \widetilde{\Omega} \times \widetilde{n}_{P''},
$$

by means of which the solutions of systems (33) can be expressed as follows

$$
\begin{aligned}
\widetilde{P}_< &= c\widetilde{\Omega} + s\{\cos[\omega''(\chi - \chi'')]\widetilde{m}_{P''} \\
&\quad - \sin[\omega''(\chi - \chi'')]\widetilde{n}_{P''}\}, \\
\widetilde{Q} < &= c\widetilde{\Omega} - s\{\cos[\omega''(\chi - \chi'')]\widetilde{m}_{P''} \\
&\quad - \sin[\omega''(\chi - \chi'')]\widetilde{n}_{P''}\}, \\
\omega'' &= \omega|\widetilde{P}'' + \widetilde{Q}''|, \quad c = \cos\frac{(\widetilde{P}''\widetilde{Q}'')}{2}, \\
s &= \sin\frac{(\widetilde{P}''\widetilde{Q}'')}{2}, \quad \chi'' = -\ln|t''|.
\end{aligned}
\quad \text{(A3)}
$$

This solution describes an infinitely fast rotation of the charges in the neighborhood of their meeting point, if they are treated as a function of time, and we have a rotation with a constant frequency ω'' in the logarithmic variables χ. To continue the solution beyond the singularity for positive times, we assume that in the time interval $-t_{\min} < t < t_{\min}$, the particle charge vector does not change. The time scale $t_{\min}$ is of artificial character and can be chosen arbitrarily small, in principle. Without retardation the solution of Eq. (34) at $t > t_{\min}$ can be written as

$$
\begin{aligned}
\widetilde{P}_> &= c\widetilde{\Omega} + s\{\cos[\omega''(\chi - \chi^*)]\widetilde{m}_{P''} \\
&\quad + \sin[\omega''(\chi - \chi^*)]\widetilde{n}_{P''}\}, \\
\widetilde{Q}_> &= c\widetilde{\Omega} - s\{\cos[\omega''(\chi - \chi^{**})]\widetilde{m}_{P''} \\
&\quad + \sin[\omega''(\chi - \chi^{**})]\widetilde{n}_{P''}\},
\end{aligned} \quad (A4)
$$

where $\chi = -\ln t$, χ^*, χ^{**} are arbitrary phases to be defined by the known values of the charge vectors on the left end of the segment $-t_{\min}$

$$
\begin{aligned}
\widetilde{P}_<(-t_{\min}) &= \widetilde{P}_>(t_{\min}), \\
\widetilde{Q}_<(-t_{\min}) &= \widetilde{Q}_>(t_{\min}).
\end{aligned}
$$

Comparing Eqs. (A3) and (A4), one can obtain relations between the phase χ'' and phases χ^* and χ^{**}. It is seen that it is convenient to put the time $t_{\min}$ in such a way that $\sin[\omega''(\chi_{\min} - \chi'')] = 0$, with $\chi_{\min} = -\ln t_{\min}$; i.e., $\chi_{\min} = 2\pi n/\omega'' + \chi''$, where n is an integer number. Then one can put $\chi^* = \chi^{**} = \chi''$. As a result, the expression for positive times will not be overloaded by formal phase shifts and at the same time an arbitrarily small time scale $t_{\min}$ can be chosen. Thus, the solution for the time scale $t_{\min} < t < |t''|$ has been obtained. As a result, we can see that

$$
\begin{aligned}
\widetilde{P}_<(t'') &= \widetilde{P}_>(|t''|) = \widetilde{P}'', \\
\widetilde{Q}_<(t'') &= \widetilde{Q}_>(|t''|) = \widetilde{Q}'',
\end{aligned}
$$

i.e., in this approximation the phase shift is not observed, and the color charge vector at the exit from the scale t'' coincides with that at its entrance.

(iii) The time $-t'' < t \leqslant t_{\text{out}}$, $t_{\text{out}} < t$. We continue the approximate solution to larger times in such a way that a change of the color rotation regime on the scale $t_{\text{out}} \sim |t'|$ should occur symmetrically with respect to the negative time and the rotation should stop when the scale $t \sim |T|$ is reached. This solution for the positive time can be written in the form [a change of the sign in this system in comparison with Eq. (A2) should be mentioned]

$$
\begin{aligned}
\widetilde{P}_> &= \cos\theta_o \widetilde{Q}_o + \sin\theta_o\{\cos[\omega(\chi - \chi_o^*)]\widetilde{m}_{P_o} \\
&\quad + \sin[\omega(\chi - \chi_o^*)]\widetilde{n}_{P_o}\}, \quad |t''| \leqslant t < |t'|, \\
\widetilde{Q}_> &= \cos\theta_o \widetilde{P}_o + \sin\theta_o\{\cos[\omega(\chi - \chi_o^{**})]\widetilde{m}_{Q_o} \\
&\quad - \sin[\omega(\chi - \chi_o^{**})]\widetilde{n}_{Q_o}\}, \quad (A5)
\end{aligned}
$$

with yet unknown basis vectors

$$
\begin{aligned}
&\widetilde{Q}_o, \quad \widetilde{n}_{P_o} = \frac{\widetilde{P}_o \times \widetilde{Q}_o}{\sin\theta_o}, \quad \widetilde{m}_{P_o} = \widetilde{Q}_o \times \widetilde{n}_{P_o}, \\
&\widetilde{P}_o, \quad \widetilde{n}_{Q_o} = -\widetilde{n}_{P_o}, \quad \widetilde{m}_{Q_o} = \widetilde{P}_o \times \widetilde{n}_{Q_o},
\end{aligned}
$$

on which the solution is spanned and with the corresponding phases χ_o^*, χ_o^{**}. Here $\cos\theta_o = (\widetilde{P}_o\widetilde{Q}_o)$. This information should be restored using the available $\widetilde{P}_>(|t''|) = \widetilde{P}''$, $\widetilde{Q}_>(|t''|) = \widetilde{Q}''$. The vector product $\widetilde{P}'' \times \widetilde{Q}''$ gives another condition in addition to the relations (A5). Applying the vector algebra rules, these relations can be presented in the matrix form

$$
\begin{aligned}
a_{11}\widetilde{P}_o + a_{12}\widetilde{Q}_o + a_{13}\widetilde{n}_{P_o} &= \widetilde{P}'', \\
a_{21}\widetilde{P}_o + a_{22}\widetilde{Q}_o + a_{23}\widetilde{n}_{P_o} &= \widetilde{Q}'', \\
a_{31}\widetilde{P}_o + a_{32}\widetilde{Q}_o + a_{33}\widetilde{n}_{P_o} &= \widetilde{P}'' \times \widetilde{Q}'', \quad (A6)
\end{aligned}
$$

with the coefficients

$$
\begin{aligned}
a_{11} &= c_1, \quad a_{12} = c(1 - c_1), \quad a_{13} = s_1, \\
a_{21} &= c(1 - c_2), \quad a_{22} = c_2, \quad a_{23} = -s_2, \\
a_{31} &= (\alpha - \beta c)/s, \quad a_{32} = (\beta - \alpha c)/s, \quad a_{33} = \gamma s,
\end{aligned}
$$

where the following notation is used:

$$
\begin{aligned}
\alpha &= -c_2 s_1 - c(1 - c_1)s_2, \\
\beta &= c_1 s_2 + c(1 - c_2)s_1, \\
\gamma &= c_1 c_2 - c^2(1 - c_1)(1 - c_2), \\
c &= \cos\theta_o = (\widetilde{P}_o\widetilde{Q}_o), \\
s &= \sin\theta_o, \quad c_1 = \cos\theta_o^*, \\
s_1 &= \sin\theta_o^*, \quad \theta_o^* = \omega(\chi'' - \chi_o^*), \\
c_2 &= \cos\theta_o^{**}, \quad s_2 = \sin\theta_o^{**}, \quad \theta_o^{**} = \omega(\chi'' - \chi_o^{**}).
\end{aligned}
$$

Now, if all the phases are known, then one can find $\widetilde{P}_o$, $\widetilde{Q}_o$ using the inverse matrix A^{-1}.

In order to determine the phases, we use an important relation for the scalar product of vectors $\widetilde{P}''$ and $\widetilde{Q}''$

$$
\begin{aligned}
(1 - c_1)(1 - c_2)c^3 &+ (c_1 + c_2 - c_1 c_2)c - s_1 s_2 \\
&= (\widetilde{P}''\widetilde{Q}''). \quad (A7)
\end{aligned}
$$

Numerical analysis with the coefficients c_1, c_2 (s_1, s_2) shows that the resulting cubic equations for the cosine of the angle between the vectors $\widetilde{P}_o$ and $\widetilde{Q}_o$ has one real and two complex conjugate roots. The real root does not always satisfy the restriction $|c| < 1$, i.e., in general all of the coefficients c_1, c_2, (s_1, s_2), and c should be consistent. The boundaries of the acceptable region are defined by setting $c = \pm 1$, then

$$
\pm(1 \mp s_1 s_2) = (\widetilde{P}''\widetilde{Q}'').
$$

In particular, for the parallel and antiparallel vectors $\widetilde{P}''$ and $\widetilde{Q}''$ we have $s_1 = s_2 = 0$. For an approximate solution we can restrict ourselves to a particular case $s_1 = s_2 = 0$ just as we did in choosing the phase $\chi_{\min}$. Then for the phase one can get

$$
\omega(\chi'' - \chi_o^*) = 0 + 2\pi n, \quad \omega(\chi'' - \chi_o^*) = \pi + 2\pi n,
$$

where n is an integer. Similar relations hold for the phase χ_o^{**}. The time scale, when the rotation around the constant charge vector of the particle partner stops, is defined by the condition $t_{\text{out}} = e^{-\chi_o^*}$. The analyzed cases show that for the considered particle velocities (with reasonable accuracy) will fall at the scale of $|t'|$, if the phase is chosen as $\chi_o^* = \chi_o^{**} = \chi'' - \pi/\omega$. This regime is approximately applied when $m/\mathcal{E} < 10^{-1.5}$ and it gets better with an increase in energy reaching the required scale. In principle, nothing prevents installing the time t_{out} also for moderate relativistic velocities, because at this scale $\sim t'$ the change in color charges is insignificant, as compared to the scale t''. With this choice of the phase, Eq. (A7) takes the form

$$4c^3 - 3c = (\widetilde{P}''\widetilde{Q}'').$$

This equation has one real root, which always satisfies the condition $|c| < 1$, and two conjugated imaginary roots. Now with the known coefficients c_1, c_2, (s_1, s_2), and c, one can find the vectors of the particles that define the basic three vectors, which are spanned over the solutions for positive time scales t_{out} and $|T|$. The equation set (A6) for particular cases interested takes the form

$$-\widetilde{P}_o + 2c\widetilde{Q}_o = \widetilde{P}'', \quad 2c\widetilde{P}_o - \widetilde{Q}_o = \widetilde{Q}''.$$

From here we get the solutions

$$\widetilde{P}_o = \frac{1}{4c^2 - 1}\widetilde{P}'' + \frac{2c}{4c^2 - 1}\widetilde{Q}'',$$

$$\widetilde{Q}_o = \frac{2c}{4c^2 - 1}\widetilde{P}'' + \frac{1}{4c^2 - 1}\widetilde{Q}''.$$

The explicit expressions provide an approximate solution of Eq. (32) continuous in time, which can be applied to the entire time axis.

2. Color charge and dipole

As before we assume that particles begin to feel the presence of the third-particle color charge when approaching the distance D estimated as 1 fm. The signal of the presence of the charge $\widetilde{P}$ arrives at the second particle at time t_2', and at the third one at $t_3' = t_2' + t_3$. We ignore the time difference between t_2' and t_3' (due to the Lorentz contraction), i.e., the charges of the second and third particles do not change up to the time t_2'. With the same degree of accuracy, the signals from the second and third charges will come to the first particle at the time t_1'. Until this point the first particle charge $\widetilde{P}$ does not change in time. Then the charges rotate with respect to the constant charge vector, which the particles had at the entrance in the interaction zone. For these times the compatibility conditions (A5) become

$$\dot{\widetilde{P}} = \omega\left[\frac{1}{|t|} - \frac{1}{|t - t_3|}\right]\widetilde{Q}_T \times \widetilde{P},$$

$$\dot{\widetilde{Q}}_2 = \omega\frac{1}{|t|}\widetilde{P}_T \times \widetilde{Q}_2 - \omega_\parallel\frac{1}{t_3}\widetilde{Q}_T \times \widetilde{Q}_2, \qquad \text{(A8)}$$

$$\dot{\widetilde{Q}}_3 = \omega\frac{1}{|t - t_3|}\widetilde{P}_T \times \widetilde{Q}_3 - \omega_\parallel\frac{1}{t_3}\widetilde{Q}_T \times \widetilde{Q}_3,$$

with $\omega_\parallel = \frac{\alpha_g(1 - w^2)}{v + w}$. From this system one can conclude that due to the factor of $\omega_\parallel$ the charges of $\widetilde{Q}_2$ and $\widetilde{Q}_3$ can be considered as mutually opposite well away from the meeting point (as well as at the entrance to the interaction zone), in particular, until the scale t', the dynamics of color charges is described by a simplified system of the two equations

$$\dot{\widetilde{P}} = \omega\left[\frac{1}{|t|} - \frac{1}{|t - t_3|}\right]\widetilde{Q}_T \times \widetilde{P},$$

$$\dot{\widetilde{Q}} = \omega\frac{1}{|t|}\widetilde{P}_T \times \widetilde{Q}, \qquad \text{(A9)}$$

$\widetilde{Q}_2 = \widetilde{Q}$, $\widetilde{Q}_3 = -\widetilde{Q}$. Comparing this set of equations with Eqs. (32) we get a solution in the form

$$\widetilde{P}_< = \cos\theta\,\widetilde{Q}_T + \sin\theta\big\{\cos[\omega(\eta - \eta_1')]\widetilde{m}_{P_T}$$
$$- \sin[\omega(\eta - \eta_1')]\widetilde{n}_{P_T}\big\}, \quad t_1' \leqslant t < t'',$$

$$\widetilde{Q}_< = \cos\theta\,\widetilde{P}_T + \sin\theta\big\{\cos[\omega(\chi - \chi_2')]\widetilde{m}_{Q_T}$$
$$- \sin[\omega(\chi - \chi_2')]\widetilde{n}_{Q_T}\big\}, \quad t_2' \leqslant t < t'',$$

where

$$\eta = \chi - \psi, \quad \chi = -\ln|t|, \quad \psi = -\ln|t - t_3|,$$

with the initial data on the scale t'. In this case, the dipole charges act on the color charge of the first particle weaker than a single color charge because the contributions compensate each other. This scheme is equivalent to item (i) of the previous section, and describes the behavior of charges for times $t < T$, $T \leqslant t < t''$.

As in the case of the two color charges let us take as an acceptable approximation to the exact solution the matching of the solution on the scale t'', which neglects the retardation, and the above solutions for the time scale larger than t'. In the meeting area the charges of the first and second particles are described by the familiar equations

$$\dot{\widetilde{P}} = \omega\frac{1}{|t|}\widetilde{Q}_2 \times \widetilde{P}, \quad \dot{\widetilde{Q}}_2 = \omega\frac{1}{|t|}\widetilde{P} \times \widetilde{Q}_2. \quad \text{(A10)}$$

In contrast to the singular behavior dictated by this system, the charge of the third particle obeys

$$\dot{\widetilde{Q}}_3 \simeq \omega\frac{1}{t_3}\widetilde{P}_T \times \widetilde{Q}_3.$$

In many applications the time scale t'' is so small that in this interval the color vector $\widetilde{Q}_3$ can even be taken as a constant. As was mentioned in the section devoted to the two color charges, after the singularity point for a positive time $t = |t''|$ the charges take the same position in the color space as at the entrance to the singularity zone. Therefore, the continuation to larger positive times used for the two color charges holds valid in the color-dipole case, the color charge dynamics being described by the simplified system of equations (A9). The initial data are defined by the obvious matching of the condition with a singular solution at the time $t = |t''|$, which we do not present here. It is clear that the same considerations of the behavior of color charges can be applied to the meeting point

of the first charge with the third particle on the scale of t'' in the neighborhood of t_3.

$$\dot{\widetilde{P}} = \omega \frac{1}{|t - t_3|} \widetilde{Q}_3 \times \widetilde{P}, \quad \dot{\widetilde{Q}}_3 = \omega \frac{1}{|t - t_3|} \widetilde{P} \times \widetilde{Q}_3. \quad (A11)$$

In its turn, the charge vector of the second particle $\widetilde{Q}_2$ can be considered in this segment as constant. As in item (ii) of the previous section for the times $t'' \leqslant t \leqslant -t''$, here for the times $t'' \leqslant t - t_3 \leqslant -t''$ one should construct the appropriate three basic vectors based on the continuous vector $\widetilde{P}(t_3 + t'') + \widetilde{Q}_3(t_3 + t'')$ and introduce an additional time scale $t_{\min}$, which is defined by the relation $\chi_{\min} = 2\pi n/\omega_{t_3+t''} + \chi''$, $\Omega_{t_3+t''} = |\widetilde{P}(t_3 + t'') + \widetilde{Q}_3(t_3 + t'')|$. In this way we obtain solutions analogous to those in item (ii) but for the case of two color charges at the meeting points of the particles 1-2 and 1-3.

The continuation of the solution to larger times should be carried out by analogy with item (iii) of the previous section, i.e., first, to construct the description of charges on the scale $-t'$, then on the scale of $t_3 + t'$ and so on, up to the scale $t_3 + t''$ where there is a meeting of the first and third particle and the behavior of charges is singular. But such a meticulous description apparently is not needed if approximate solutions are considered. So we just accept that the passage to the regime of rotation around constant vectors of color charges of particle partners at the exit from the interaction zone occurs somewhere on the scale t_3. Such a solution of (A9) is as follows:

$$\widetilde{P}_> = \cos \theta_o \widetilde{Q}_o + \sin \theta_o \big\{ \cos[\omega(\eta - \eta_o^*)] \widetilde{m}_{P_o}$$
$$+ \sin[\omega(\eta - \eta_o^*)] \widetilde{n}_{P_o} \big\}, \quad |t''| \leqslant t < t_{\text{out}},$$
$$\widetilde{Q}_> = \cos \theta_o \widetilde{P}_o + \sin \theta_o \big\{ \cos[\omega(\chi - \chi_o^{**})] \widetilde{m}_{Q_o}$$
$$- \sin[\omega(\chi - \chi_o^{**})] \widetilde{n}_{Q_o} \big\},$$

where as in the previous section, one should determine the basic three vectors and phases using available information on the scales t'', i.e., $\widetilde{P}''$, $\widetilde{Q}''$. The corresponding systems of equations have the form (A6) and (A7), where the variable substitution $\chi \to \eta$ should be made for variables related with the vector of the first particle charge $\widetilde{P}$. As was noted in the previous section, the easiest version of the inverse problem of reconstruction of the basis vectors and phases would be appropriate if this choice of variables gives $s_1 = s_2 = 0$. An analysis shows that for the problem of the particle and the dipole one can take

$$\omega(\eta'' - \eta_o^*) = 2\pi, \quad \omega(\chi'' - \chi_o^{**}) = \pi.$$

With this choice of phases, going on to large positive times occurs somewhere on the scale of t_3 for the first particle and on the scale t_2' for the second one

$$t_{o1} = \frac{t_3}{1 - e^{-x_{o1}}}, \quad x_{o1} = \frac{2\pi}{\omega} - \eta''$$
$$t_{o2} = e^{-x_{o2}}, \quad x_{o2} = \chi'' - \frac{\pi}{\omega}.$$

As mentioned above, there is no sense in complicating the task by better matching the transition regime for asymptotically large times. Now Eq. (A7) becomes ($c_1 = 1$, $c_2 = -1$)

$$c = (\widetilde{P}'' \widetilde{Q}'').$$

The system of equations (A6) in which we are particularly interested takes the form

$$\widetilde{P}_o = \widetilde{P}'', \quad 2c \widetilde{P}_o - \widetilde{Q}_o = \widetilde{Q}''.$$

In this way we complete the description referred to the item (iii) for the problem of two color charges. The whole procedure to obtain approximate solutions for the system of compatibility equations (36) is reduced to the description of the behavior of two basic charges, since the partner charge in a dipole pair can be considered as adjusted. The passage for a short time on the scale t'' to a singular rotation regime is not accompanied by a change in phase.

We have missed some interesting effects of the arrival of the signal to the particle partner in the dipole from the meeting point of two other particles. In Fig. 9, the marked point 12 corresponds to the light signal coming from the meeting of the first and second charges to the third color charge. In these times on the scale t'' the charge of the third particle is described by the equation

$$\dot{\widetilde{Q}}_3 \simeq \omega \frac{1}{t_3} \widetilde{P} \times \widetilde{Q}_3, \quad (A12)$$

where the charge of the first particle $\widetilde{P}$ is rapidly changing in a singular manner. Unfortunately, it is difficult to derive analytical expressions describing the behavior of the color charge of the third particle, and in this paper we simply ignore this important, but short, episode. It is also important to note in turn that a signal about events that happened to the third charge prior to the collision of the first charge with the third particle in time reaches the first particle. Then, a signal will come to the third particle even before the meeting of the first and the third particles, and so on. There is some danger that we are not able to control the behavior of charges at the second meeting point because one should trace the ladder of events up to the meeting point (we have not depicted in Fig. 9 an appropriate sequence of signals similar to those shown in Fig. 2). However, it is noteworthy that these processes should not change too much the color charge phase since the first signal comes on the scale $t_3 \sim m/\mathcal{E}$, and the second one occurs on the scale $t_3 \times t'' \sim m^5/\mathcal{E}^5$, while the merging of solutions takes place on the scale t''.

3. Two color dipoles

We discard a detailed prescription for obtaining approximate solutions, as was done in the previous sections. Let us write down directly the simplified system of equations, which allows us to describe the behavior of color charges for large times,

$$\dot{\widetilde{P}} = \omega \left[\frac{1}{|t|} - \frac{1}{|t - t_3|} \right] \widetilde{Q}_T \times \widetilde{P},$$
$$\dot{\widetilde{Q}} = \omega \left[\frac{1}{|t|} - \frac{1}{|t - t_4|} \right] \widetilde{P}_T \times \widetilde{Q}, \quad (A13)$$

where $\widetilde{P}_1 = \widetilde{P}$, $\widetilde{P}_4 = -\widetilde{P}$, $\widetilde{Q}_2 = \widetilde{Q}$, $\widetilde{Q}_3 = -\widetilde{Q}$. One should specify that under construction of approximate solutions there are an additional basic three vectors by means of which solutions at the meeting point of particles are built. One should also introduce the appropriate set of times $t_{\min}$, where formally singular solutions are matched. On a time scale t'

the solution of the system (A13) has the form

$$
\begin{aligned}
\widetilde{P}_< &= \cos\theta\,\widetilde{Q}_T + \sin\theta\big\{\cos[\omega(\eta - \eta_1')]\widetilde{m}_{P_T} \\
&\quad - \sin[\omega(\eta - \eta_1')]\widetilde{n}_{P_T}\big\}, \quad t_1' \leqslant t < t'',
\end{aligned}
$$

$$
\begin{aligned}
\widetilde{Q}_< &= \cos\theta\,\widetilde{P}_T + \sin\theta\big\{\cos[\omega(\zeta - \zeta_2')]\widetilde{m}_{Q_T} \\
&\quad - \sin[\omega(\zeta - \zeta_2')]\widetilde{n}_{Q_T}\big\}, \quad t_2' \leqslant t < t'',
\end{aligned}
$$

where

$$
\begin{aligned}
\eta &= \chi - \psi, \quad \zeta = \chi - \xi, \quad \chi = -\ln|t|, \\
\psi &= -\ln|t - t_3|, \quad \xi = -\ln|t - t_4|,
\end{aligned} \tag{A14}
$$

with the initial data taken on the scale t'. The passage of approximate solutions from the scale $|t''|$ to large positive times is described by the solution of the form

$$
\begin{aligned}
\widetilde{P}_> &= \cos\theta_o\,\widetilde{Q}_o + \sin\theta_o\big\{\cos[\omega(\eta - \eta_o^*)]\widetilde{m}_{P_o} \\
&\quad + \sin[\omega(\eta - \eta_o^*)]\widetilde{n}_{P_o}\big\}, \quad |t''| \leqslant t < t_{\text{out}},
\end{aligned}
$$

$$
\begin{aligned}
\widetilde{Q}_> &= \cos\theta_o\,\widetilde{P}_o + \sin\theta_o\big\{\cos[\omega(\zeta - \zeta_o^{**})]\widetilde{m}_{Q_o} \\
&\quad - \sin[\omega(\zeta - \zeta_o^{**})]\widetilde{n}_{Q_o}\big\},
\end{aligned}
$$

where the three basic vectors and phase are determined by the conditions $s_1 = s_2 = 0$ discussed above. Under these conditions one can avoid solutions of the complicated inverse problem of the restoration of basic triple vectors using the initial data on the scale t''. In the case of two dipoles one can take

$$
\omega(\eta'' - \eta_o^*) = 2\pi, \quad \omega(\zeta'' - \zeta_o^{**}) = 2\pi.
$$

With this choice of the phase the passage to large positive times for the first and fourth particle occurs somewhere on the scale t_4 and on the scale t_3 for the second and third particle

$$
\begin{aligned}
t_{o1} &= \frac{t_3}{1 - e^{-x_{o1}}}, \quad x_{o1} = \frac{2\pi}{\omega} - \eta'', \\
t_{o2} &= \frac{t_4}{1 - e^{-x_{o2}}}, \quad x_{o2} = \frac{2\pi}{\omega} - \zeta''.
\end{aligned} \tag{A15}
$$

Accordingly, in the case of two dipoles the passage to large positive times is more consistent than in the particle-dipole case. Now Eq. (A7) becomes ($c_1 = 1$, $c_2 = 1$)

$$
c = (\widetilde{P}''\widetilde{Q}'').
$$

For a particular case considered the system (A6) is reduced to

$$
\widetilde{P}_o = \widetilde{P}'', \quad \widetilde{Q}_o = \widetilde{Q}''.
$$

Thus, the approximate solution on the entire time axis has been constructed.

---

[1] I. Arsene *et al.*, Nucl. Phys. A **757**, 1 (2005).

[2] B. B. Back *et al.*, Nucl. Phys. A **757**, 28 (2005).

[3] J. Adams *et al.*, Nucl. Phys. A **757**, 101 (2005).

[4] K. Adcox *et al.*, Nucl. Phys. A **757**, 184 (2005).

[5] K. Aamodt *et al.*, Phys. Rev. Lett. **105**, 252302 (2010).

[6] E. Shuryak, Prog. Part. Nucl. Phys. **53**, 273 (2004).

[7] A. Peshier and W. Cassing, Phys. Rev. Lett. **94**, 172301 (2005).

[8] T. Hirano and M. Gyulassy, Nucl. Phys. A **769**, 71 (2006).

[9] U. Heinz and V. Kolb, Nucl. Phys. A **702**, 269 (2002).

[10] P. Romatschke and U. Romatschke, Phys. Rev. Lett. **99**, 172301 (2007).

[11] U. Heinz and R. Snellings, Annu. Rev. Nucl. Part. Sci. **63**, 123 (2013).

[12] M. Miller and R. Snellings, arXiv:nucl-ex/0312008.

[13] O. Socolowski, F. Grassi, Y. Hama, and T. Kodama, Phys. Rev. Lett. **93**, 182301 (2004).

[14] P. Sorensen, J. Phys. G **37**, 094011 (2010).

[15] B. Alver and G. Roland, Phys. Rev. C **81**, 054905 (2010).

[16] V. D. Toneev, V. P. Konchakovski, V. Voronyuk, E. L. Bratkovskaya, and W. Cassing, Phys. Rev. C **86**, 064907 (2012).

[17] B. Schenke, S. Jeon, and C. Gale, J. Phys. G **38**, 124169 (2011); Phys. Rev. C **85**, 024901 (2012).

[18] V. P. Konchakovski, E. L. Bratkovskaya, W. Cassing, V. D. Toneev, S. A. Voloshin, and V. Voronyuk, Phys. Rev. C **85**, 044922 (2012).

[19] P. K. Kovtun, D. T. Son, and A. O. Starinets, Phys. Rev. Lett. **94**, 111601 (2005).

[20] S. Mattiello and W. Cassing, Eur. Phys. J. C **70**, 243 (2010).

[21] S. Plumari, A. Puglisi, F. Scardina, and V. Greco, Phys. Rev. C **86**, 054902 (2012).

[22] A. S. Khvorostukhin, V. D. Toneev, and D. N. Voskresensky, Phys. Rev. C **83**, 035204 (2011); Nucl. Phys. A **843**, 106 (2010).

[23] V. Ozvenchuk, O. Linnyk, M. I. Gorenstein, E. L. Bratkovskaya, and W. Cassing, Phys. Rev. C **87**, 064903 (2013).

[24] M. Bluhm, B. Kämpfer, and K. Redlich, Phys. Rev. C **84**, 025201 (2011).

[25] K. Zhang, J. Song, and F. L. Shao, Phys. Rev. C **86**, 014906 (2012).

[26] T. Lappi and L. McLerran, Nucl. Phys. A **772**, 200 (2006); T. Lappi, Int. J. Mod. Phys. E **20**, 1 (2011).

[27] W. Cassing and E. L. Bratkovskaya, Nucl. Phys. A **831**, 215 (2009).

[28] E. L. Bratkovskaya *et al.*, Nucl. Phys. A **856**, 162 (2011).

[29] V. D. Toneev, V. Voronyuk, E. L. Bratkovskaya, W. Cassing, V. P. Konchakovski, and S. A. Voloshin, Phys. Rev. C **85**, 034910 (2012).

[30] V. P. Konchakovski, E. L. Bratkovskaya, W. Cassing, V. D. Toneev, and V. Voronyuk, Phys. Rev. C **85**, 011902 (2012).

[31] O. Linnyk, W. Cassing, J. Manninen, E. L. Bratkovskaya, and C. M. Ko, Phys. Rev. C **85**, 024910 (2012); O. Linnyk, E. L. Bratkovskaya, V. Ozvenchuk, W. Cassing, and C. M. Ko, *ibid.* **84**, 054917 (2011); O. Linnyk, W. Cassing, J. Manninen, E. L. Bratkovskaya, P. B. Gossiaux, J. Aichelin, T. Song, and C. M. Ko, *ibid.* **87**, 014905 (2013).

[32] I. N. Mishustin and K. A. Lyakhov, Phys. At. Nucl. **75**, 371 (2012).

[33] L. V. Gribov, E. M. Levin, and M. G. Ryskin, Phys. Rep. **526**, 165 (1983).

[34] F. Gelis, E. Iancu, J. Jalilian-Marian, and R. Venugopalan, Annu. Rev. Nucl. Part. Sci. **60**, 463 (2010); E. Iancu and

R. Venugopalan, in *Quark Gluon Plasma*, edited by R. Hwa and X. N. Wang (World Scientific, Singapore, 2003); H. Weigert, Prog. Part. Nucl. Phys. **55**, 461 (2005).

[35] E. Kuraev, L. Lipatov, and V. Fadin, Sov. Phys. JETP **45**, 199 (1977); Y. Balitsky and L. Lipatov, Sov. J. Nucl. Phys. **28**, 822 (1978).

[36] L. McLerran and R. Venugopalan, Phys. Rev. D **49**, 2233 (1994); **49**, 3352 (1994); **50**, 2225 (1994).

[37] J. Jalilian-Marian, A. Kovner, L. McLerran, and H. Weigert, Phys. Rev. D **55**, 5414 (1997); J. Jalilian-Marian, A. Kovner, A. Leonidov, and H. Weigert, Nucl. Phys. B **504**, 415 (1997); Phys. Rev. D **59**, 034007 (1999); **59**, 099903(E) (1999); E. Iancu, A. Leonidov, and L. D. McLerran, Nucl. Phys. A **692**, 583 (2001).

[38] A. Dumitru and L. D. McLerran, Nucl. Phys. A **700**, 492 (2002); J. P. Blaizot, F. Gelis, and R. Venugopalan, *ibid.* **743**, 13 (2004); **743**, 57 (2004); D. Kharzeev, E. Levin, and L. McLerran, Phys. Lett. B **561**, 93 (2003); J. Jalilian-Marian, Y. Nara, and R. Venugopalan, *ibid.* **577**, 54 (2003); D. Kharzeev, Y. V. Kovchegov, and K. Tuchin, Phys. Rev. D **68**, 094013 (2003); Phys. Lett. B **599**, 23 (1998); A. Dumitru, A. Hayashigaki, and J. Jalilian-Marian, Nucl. Phys. A **765**, 464 (2006).

[39] J. L. Albacete, J. Phys. G: Nucl. Part. Phys. **38**, 124006 (2011).

[40] Ch. Gale, S. Jeon, and B. Schenke, Int. J. Mod. Phys. A **28**, 1340011 (2013).

[41] B. Schenke, P. Tribedy, and R. Venugopalan, Phys. Rev. Lett. **108**, 252301 (2012); Phys. Rev. C **86**, 034908 (2012).

[42] C. Gale, S. Jeon, B. Schenke, P. Tribedy, and R. Venugopalan, Phys. Rev. Lett. **110**, 012302 (2013).

[43] V. Voronyuk, V. D. Toneev, W. Cassing, E. L. Bratkovskaya, V. P. Konchakovski, and S. A. Voloshin, Phys. Rev. C **83**, 054911 (2011).

[44] K. Tuchin, Adv. High Energy Phys. **2013**, 490495 (2013).

[45] J. Bloczynski, X.-G. Huang, X. Zhang, and J. Liao, Phys. Lett. B **718**, 1529 (2013).

[46] I. N. Mishustin and J. I. Kapusta, Phys. Rev. Lett. **88**, 112501 (2002); I. N. Mishustin and K. A. Lyakhov, Phys. Rev. C **76**, 011603(R) (2007).

[47] L. D. Landau and E. M. Lifshitz, *The Classical Theory of Fields*, Fourth English Edition, Course of Theoretical Physics, Vol. 2 (Butterworth-Heinemann, Oxford, 1994); Yu. P. Terletsky and Yu. P. Rybakov, *Electrodynamics* (High School, Moscow, 1990) (in Russian).

[48] F. Rohrlich, *Classical Charged Particles*, 3rd ed. (World Scientific, Singapore, 2007).

[49] S. K. Wong, Nuovo Cimento A **65**, 689 (1970).

[50] I. B. Khriplovich, JETF **74**, 37 (1978) (in Russian).

[51] V. V. Goloviznin, S. V. Molodtsov, and A. M. Snigirev, Yad. Fiz. **56**, 123 (1993) (in Russian).

[52] A. F. Matveev and S. V. Molodtsov, Differ. Equat. **29**, 1533 (1993) (in Russian).

[53] J. Mandula, Phys. Rev. D **14**, 3497 (1976); Phys. Lett. B **67**, 175 (1977); **69**, 495 (1977).

[54] L. E. Elsgolts and S. B. Norkin, *Introduction to the Theory of Differential Equations with Deviating Argument* (Nauka, Moscow, 1971) (in Russian); A. D. Myshkis, *Linear differential equations with delay* (Nauka, Moscow, 1972) (in Russian); E. Pinney, *Ordinary Differential Difference Equations* (University of California Press, Berkeley, 1958); R. Bellman and K. L. Cooke, *Differential Difference Equations* (Academic Press, Waltham, Massachusetts, 1963).

[55] Y. V. Kovchegov and D. H. Rischke, Phys. Rev. C **56**, 1084 (1997).

[56] A. H. Mueller, Nucl. Phys. B **415**, 373 (1994); **437**, 107 (1995); A. H. Mueller and B. Patel, *ibid.* **425**, 471 (1994).

[57] S. G. Matinyan, B. Müller, and D. H. Rischke, Phys. Rev. C **57**, 1927 (1998).

[58] G. M. Zinovjev and S. V. Molodtsov, Theor. Math. Phys. **146**, 221 (2006); Phys. Atom. Nucl. **70**, 1136 (2007).

[59] S. V. Molodtsov, A. M. Snigirev, and G. M. Zinovjev, Phys. Lett. B **443**, 387 (1998); Phys. Rev. C **59**, 955 (1999).